Iron availability limits the ocean nitrogen inventory stabilizing feedbacks between marine denitrification and nitrogen fixation

J. Keith Moore[1] and Scott C. Doney[2]

Received 22 May 2006; revised 25 September 2006; accepted 15 December 2006; published 4 April 2007.

[1] Recent upward revisions in key sink/source terms for fixed nitrogen (N) in the oceans imply a short residence time and strong negative feedbacks involving denitrification and N fixation to prevent large swings in the ocean N inventory over timescales of a few centuries. We tested the strength of these feedbacks in a global biogeochemical elemental cycling (BEC) ocean model that includes water column denitrification and an explicit N fixing phytoplankton group. In the northern Indian Ocean and over longer timescales in the tropical Atlantic, we find strong stabilizing feedbacks that minimize changes in marine N inventory over timescales of ~30–200 years. In these regions high atmospheric dust/iron inputs lead to phosphorus limitation of diazotrophs, and thus a tight link between N fixation and surface water N/P ratios. Maintenance of the oxygen minimum zones in these basins depends on N fixation driven export. The stabilizing feedbacks in other regions are significant but weaker owing to iron limitation of the diazotrophs. Thus Fe limitation appears to restrict the ability of N fixation to compensate for changes in denitrification in the current climate, perhaps leading the oceans to lose fixed N. We suggest that iron is the ultimate limiting nutrient leading to nitrogen being the proximate limiting nutrient over wide regions today. Iron stress was at least partially alleviated during more dusty, glacial times, leading to a higher marine N inventory, increased export production, and perhaps widespread phosphorus limitation of the phytoplankton community. The increased efficiency of the biological pump would have contributed to the glacial drawdown in atmospheric CO_2.

Citation: Moore, J. K. and S. C. Doney (2007), Iron availability limits the ocean nitrogen inventory stabilizing feedbacks between marine denitrification and nitrogen fixation, *Global Biogeochem. Cycles*, *21*, GB2001, doi:10.1029/2006GB002762.

1. Introduction

[2] Nitrogen (N) is a key nutrient limiting oceanic biological production. Changes in the size of the N reservoir can thus change the efficiency of the biological pump, impacting atmospheric CO_2 and climate [*McElroy*, 1983; *Codispoti and Christensen*, 1985; *Falkowski*, 1997]. Other key limiting nutrients include phosphorus (P), iron (Fe), and silicon (Si) [*Redfield*, 1958; *Codispoti*, 1989; *Martin et al.*, 1991; *Dugdale and Wilkerson*, 1998]. Over geological timescales, it is argued that P, rather than N, should control production because N has a shorter residence time and may adjust to available P, erasing any deficit through N fixation [*Redfield*, 1958]. However, currently, N seems more depleted than P in surface waters over much of the oceans [*Ryther and Dunstan*, 1971; *Perry and Eppley*, 1981; *Codispoti*, 1989; *Vitousek and Howarth*, 1991; *Gruber*, 2004].

[3] Diazotrophs fix dissolved N_2 gas, this N then becomes available to other organisms and is a key source of new N [*Capone et al.*, 1997; *Karl et al.*, 2002; *Mahaffey et al.*, 2005]. Denitrification causes loss of fixed N to N_2 gas and small amounts of N_2O [*Codispoti et al.*, 2001]. Denitrification occurs only in suboxic or anoxic conditions where alternate electron receptors are utilized during remineralization of organic matter, mainly within ocean sediments and in oxygen minimum zones (OMZ). Relatively high remineralization rates, weak ventilation, and low O_2 source waters lead to OMZs [e.g., *Olson et al.*, 1993].

[4] Historically, it was believed that *Trichodesmium spp*. accounted for most pelagic N fixation. However, recently evidence has accumulated for significant N fixation by other groups, including diatom endosymbionts, croccosphera and other small unicellular diazotrophs [*Villareal*, 1992; *Zehr et al.*, 2001; *Karl et al.*, 2002; *Montoya et al.*, 2004; *Mahaffey et al.*, 2005]. Key limiting factors influencing N fixation rates include the light-mixing regime, temperature, P and Fe availability. Diazotrophs have higher Fe and energy requirements than other phytoplankton [*Berman-Frank et al.*, 2001; *Kustka et al.*, 2003a].

[5] Several lines of evidence suggest widespread Fe limitation of diazotroph growth rates and N fixation, although direct observations are limited. These include some

[1]Department of Earth System Science, University of California, Irvine, California, USA.
[2]Department of Marine Chemistry and Geochemistry, Woods Hole Oceanographic Institution, Woods Hole, Massachusetts, USA.

0886-6236/07/2006GB002762$12.00

field data [*Wu et al.*, 2003], laboratory studies in conjunction with satellite data [*Berman-Frank et al.*, 2001], and laboratory studies in conjunction with field observations [*Kustka et al.*, 2003b]. Ecosystem simulations predict widespread diazotroph Fe limitation and a strong influence of dust deposition (Fe inputs) on N fixation [*Moore et al.*, 2002b, 2004, 2006]. In the North Atlantic, where there is high dust deposition, evidence for P limitation or colimitation by Fe and P has been demonstrated [*Sañudo-Wilhelmy et al.*, 2001; *Dyhrman et al.*, 2002; *Ammerman et al.*, 2003; *Kustka et al.*, 2003b; *Mills et al.*, 2004]. Recent estimates of global N fixation rates range widely from ~100–200 TgN/yr [*Gruber and Sarmiento*, 1997; *Lee et al.*, 2002; *Karl et al.*, 2002; *Galloway et al.*, 2004; *Gruber*, 2004; *Deutsch et al.*, 2004, 2007]. These estimates are much higher than in previous decades owing to improved techniques, more comprehensive field observations and application of geochemical tracer approaches [*Michaels et al.*, 1996; *Gruber and Sarmiento*, 1997; *Mahaffey et al.*, 2005] (see *Hansell et al.* [2004] for a dissenting view).

[6] Global denitrification estimates have also increased dramatically to ~200–450 TgN/yr [*Codispoti*, 1989; *Middleburg et al.*, 1996; *Codispoti et al.*, 2001; *Brandes and Devol*, 2002; *Gruber*, 2004]. Water column denitrification rates are sensitive to variations in OMZ volume and the sinking organic flux from surface waters [*Codispoti*, 1989]. Water column denitrification results in strong fractionation of N isotopes leaving behind ^{15}N enriched nitrate, while sedimentary denitrification results in weak fractionation as all of the available nitrate is typically consumed [*Brandes and Devol*, 2002]. N fixation introduces isotopically light fixed N to the oceans, with $\delta^{15}N$ close to atmospheric values. Thus N isotope observations help constrain the marine N cycle.

[7] The relative concentrations of inorganic N and P in the oceans, when combined with circulation estimates, can also constrain the N cycle. N fixation and denitrification cause deviations in the excess N tracer (or N*) that relates inorganic N and P concentrations relative to the Redfield N/P ratio of ~16 (i.e., $N^* = NO_3^- - 16 * PO_4^{3-}$ μmol kg^{-1} [*Redfield*, 1958; *Michaels et al.*, 1996; *Howell et al.*, 1997; *Gruber and Sarmiento*, 1997]). *Gruber and Sarmiento* [1997] used large-scale N* distributions in the North Atlantic to estimate a basin N fixation rate of 28 TgN/yr, extrapolated globally to ~110 TgN/yr. *Deutsch et al.* [2001] studied N* patterns in the Pacific, estimating N fixation of 59 TgN/yr. *Deutsch et al.* [2007] used observed nutrient distributions with an ocean circulation model to diagnose global N fixation at 140 TgN/yr, finding distributions consistent with *Trichodesmium* biogeography, including elevated N fixation in the subtropical gyres, but also in proximity to water column denitrification zones.

[8] The recent higher estimates for both N fixation and denitrification mark them as the dominant source and sink terms. The larger rates imply a fixed N residence time of ~1500–3000 years, down from earlier estimates of 10,000 years or more. This implies there can be significant changes in the fixed N inventory on timescales of a few hundred years. There is substantial evidence that rates of water column denitrification can vary substantially over multiple timescales with possible links to climate [*Altabet et al.*, 1995, 2002; *Ganeshram et al.*, 1995; *Suthof et al.*, 2001; *Meissner et al.*, 2005]. The factors controlling N fixation should also allow for rapid changes in global rates with changes in climate and/or dust deposition [*Gruber*, 2004; *Moore et al.*, 2006]. Stabilizing, negative feedbacks that minimize changes in N inventory over relatively short timescales have been suggested, on the basis of stable atmospheric CO_2 concentrations [*Gruber and Sarmiento*, 1997; *Gruber*, 2004] and sedimentary and modern ocean $\delta^{15}N$ constraints [*Deutsch et al.*, 2004]. *Gruber and Sarmiento* [1997] suggest imbalances in source-sink terms of 70 TgN/yr would have to be closed within ~300 years by negative feedbacks to prevent changes in pre-industrial atmospheric CO_2 larger than observed. High-deposition ice core records for the last 1000 years exhibit pre-industrial peak-to-peak variations of CO_2 of only about 6 ppm [e.g., *Siegenthaler et al.*, 2005]. Others have suggested imbalances in the source and sink terms may be the normal state as factors controlling N fixation and denitrification are only partially coupled [*Codispoti and Christensen*, 1985; *Codispoti*, 1989; *Falkowski*, 1997].

[9] *Codispoti* [1989] noted two stabilizing feedbacks: a "fast" response where increased denitrification reduces N/P ratios in surface waters leading to increased N fixation (as N depletion favors the nitrogen fixers), and a "slow" response whereby increased denitrification depletes ocean nitrate, eventually leading to a reduction in the export of organic matter, which in turn reduces denitrification rates. The terms fast and slow are relative, and the timescales should vary on the basis of ocean circulation and the distance between areas of N loss and gain. Both feedbacks would operate in the opposite sense in response to decreased denitrification. Similarly, increasing N fixation could increase export of organic material driving up denitrification (and vice versa).

[10] *Tyrrell* [1999] used an ocean box model to show the N fixation feedback could stabilize oceanic inventory, with long-term adjustment of the N inventory to the total P pool, if N/P ratios in surface waters were the only factor controlling rates of N fixation. These simulations had a steady state ocean with surface waters depleted in N relative to P (as observed in the modern ocean) with N as the "proximate" limiting nutrient, but with P as the "ultimate" limiting nutrient over long timescales. *Tyrrell* [1999] noted that other factors impacting N fixation, such as Fe, could weaken the stabilizing feedback. *Lenton and Watson* [2000] modeled the cycles of atmospheric oxygen, ocean nitrate and phosphate, with similar assumptions linking N fixation rates to nitrate deficits (relative to P). They found that N adjusted to match P levels with an N/P ratio also slightly below the Redfield value. In a "weak" N-fixation response sensitivity test (with Fe limitation as one possibility) it was possible to drive ocean N/P ratios far from the Redfield value.

[11] We examine the ocean biogeochemical response to large increases and decreases in both N fixation and water column denitrification to quantify the strength of the stabilizing feedbacks in the context of the various controls on both processes. Our study differs from previous efforts in that the ocean model is three dimensional, and diazotrophs

are explicitly simulated including all key, potentially limiting factors (phosphorus, iron, light, mixing, temperature, and interaction with the other biota). We make no explicit assumptions about the influence of N/P ratios on N fixation but rather allow them to arise from ecological competition between diazotrophs and other phytoplankton. We also examine how regional colocation or spatial separation influences the feedback processes. The computational cost associated with this more realistic simulation restricts our experiments to shorter timescales (hundreds of years rather than thousands to millions). However, the stabilizing feedbacks must operate over these short timescales if large swings in the N inventory are to be prevented.

2. Methods

[12] The Biogeochemical Elemental Cycling (BEC) ocean model simulates the biogeochemical cycling of C, O, N, P, Fe, Si, and alkalinity and four phytoplankton functional groups (diazotrophs, diatoms, pico/nano-plankton, and coccolithophores). It is based on the ecosystem model of *Moore et al.* [2002a, 2002b] coupled to a modified version of the OCMIP-2 biogeochemistry model [*Doney et al.*, 2003, 2004, 2006]. The BEC runs within the coarse-resolution POP ocean component of the Community Climate System Model (CCSM3.0) [*Collins et al.*, 2006; *Yeager et al.*, 2004]. The BEC model has been described previously by *Moore et al.* [2004, 2006] (see also auxiliary material[1]). Several parameter modifications have been made since the 2004 paper (auxiliary material Table S1). We added a water column denitrification parameterization; when O_2 concentrations fall below 4 μM, nitrate is consumed during remineralization of organic matter rather than O_2 with a stoichiometry of $C_{117}N_{16}P + 120NO_3 = > 117CO_2 + PO_4 + 68N_2$. The simulations do not include sediment denitrification, atmospheric nutrient deposition, river inputs or sediment burial. Here we focus on the last year of a 2050-year control simulation, which is used as our initial state for most experiments: Case 1 is large increase in denitrification, Case 2 is large decrease in denitrification, Case 3 is large decrease in N fixation, Case 4 is large increase in N fixation, Case 5 is large increase in denitrification with increased dust deposition to the oceans, and Case 6 is large increase in denitrification with the diazotrophs very efficient at iron uptake and utilization.

[13] The model was initialized with observed macronutrients [*Conkright et al.*, 1998], a best guess iron distribution [*Moore et al.*, 2004], and pre-industrial inorganic C and alkalinity distributions [*Key et al.*, 2004]. Winds and other climate forcings are from a late 20th century NCAR-NCEP climatology [*Large and Yeager*, 2004]. Climatological dust deposition [*Luo et al.*, 2003] delivers iron to the oceans assuming 3.5% iron by weight and a constant 2% surface solubility. Atmospheric CO_2 concentrations were set to 278 ppm for the first 2000 years of the simulation. For the last 50 years of the control and for each of our experiments, atmospheric CO_2 is simulated as a single, well-mixed box in communication with the ocean We extended the control run for an additional 200 years beyond year 2050 to quantify drift. Drifts in primary production, export, N fixation, denitrification and atmospheric CO_2 were all small relative to the changes in our perturbations (<0.5% per century). The atmospheric CO_2 declined by 1.36 ppm/century.

[14] We constrained the rates of denitrification and N fixation to be approximately in balance in the control simulation, so that ocean N inventory would not drift to an unrealistic state during the long simulation (i.e., an ocean with nitrate depleted by 50% relative to observations). In practice, this was accomplished by setting a minimum nitrate concentration below which denitrification did not occur. The minimum value was adjusted until denitrification was roughly equal to N fixation (32 μM nitrate). This is an arbitrary and unrealistic constraint, deemed necessary to prevent excessive N inventory drift. During the 2050 year simulation denitrification typically exceeded N fixation by 5–10 TgN/yr. Even this small imbalance led to a loss of 3.1% of fixed N.

[15] We designed several experiments to perturb either the source or sink of fixed N and then examined the strength and timescales of the resulting N inventory stabilizing feedbacks. In our case 1, 5, and 6 experiments, we released the artificial control on denitrification, allowing denitrification to be simply a function of O_2 concentrations and the remineralization of sinking organic material, increasing denitrification sharply. In Case 5 we also increased the atmospheric dust deposition to estimates for the Last Glacial Maximum (LGM) [*Mahowald et al.*, 2006]. This provides a reasonable, spatially realistic upper bound on dust/iron inputs, allowing us to examine feedbacks in a more Fe-replete ocean. We note that this is not an LGM simulation as atmospheric forcings, temperatures and circulation are current. In Case 2 we turn off denitrification, and in Case 3 we turn off N fixation. In Case 4, the diazotroph Fe quota was lowered (from 40 umolFe/molC to 6 umolFe/molC) so that it was identical to the other phytoplankton groups, and the diazotroph half saturation constant for Fe uptake was lowered from 0.1 nM to 0.02 nM. These somewhat unrealistic values are designed to partially relieve widespread Fe stress only for the diazotrophs, resulting in a large increase in N fixation. In Case 6 we lowered the diazotroph Fe quota and half saturation uptake constant to the model values for the small phytoplankton group (6 umolFe/molC and 0.06 nM), and released the artificial denitrification constraint. The Case 1 simulation was 430 years, and the other simulations 200 years using the control year 2050 values as initial conditions, except for Case 6 that we initialize using end values from Case 4, which has N* distributions more similar to field observations. These strong perturbations are designed to highlight the feedback responses over decadal to centennial timescales.

3. Results

[16] The control had N fixation of 58 TgN/yr and denitrification of 65 TgN/yr (Figure 1). Denitrification was dominated by the Pacific (65%) and N fixation by the Indian basin (43%). The spatial patterns for N fixation are

[1]Auxiliary material data sets are available at ftp://ftp.agu.org/apend/gb/2006gb002762. Other auxiliary material files are in the HTML.

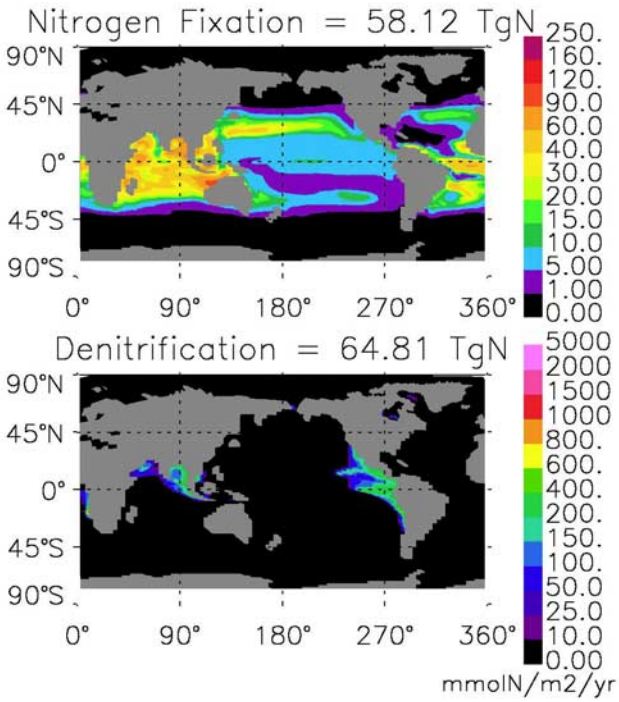

Figure 1. Nitrogen fixation and water column denitrification at the end of the control simulation (year 2050).

similar to our previous results and in relatively good agreement with limited field observations [*Moore et al.*, 2002b, 2004]. One deficiency is the low rates of N fixation in the subtropical North Atlantic where strong P-limitation restricts the growth of all phytoplankton groups. High N fixation is sometimes observed here [*Capone et al.*, 2005], likely fueled in part by dissolved organic P [*Dyhrman et al.*, 2006; *Sohm and Capone*, 2007] and mesoscale eddies [*Davis and McGillicuddy*, 2006] processes not included in the model. P limits model diazotroph growth in the North Atlantic, the low latitude and western South Atlantic, and in the northern Indian Ocean, Fe limits elsewhere at mid to low latitudes, while a temperature restriction prevents N fixation at high latitudes.

[17] Denitrification is restricted to the eastern tropical Pacific, the northern Indian ocean and a small region in the eastern S. Atlantic in qualitative agreement with in situ studies [*Codispoti et al.*, 2001]. Relative to field observations, the southern east Pacific denitrification zone extends too far north [*Codispoti and Christensen*, 1985; *Deutsch et al.*, 2004]. Denitrification appears to be underpredicted in the Arabian Sea and overpredicted in the Bay of Bengal and adjacent regions [*Howell et al.*, 1997; *Bange et al.*, 2000, 2005]. Low O_2 concentrations are observed in the eastern SW Atlantic [*Calvert and Price*, 1971] and denitrification of several TgN/yr may occur [*Codispoti et al.*, 2001; *Tyrrell and Lucas*, 2002].

[18] In Case 1, release of the denitrification constraint increased denitrification, initially exceeding 350 TgN/yr, declining below 200 TgN/yr by year 100, then gradually declining further over the 430 year simulation to 161 TgN/yr (Figure 2, includes last 20 years of the Control, and auxiliary material Table S2). The increased denitrification led to a rapid increase in N fixation (as decreasing N/P ratios in surface waters favored the diazotrophs). N fixation nearly doubled, increasing from 59 TgN/yr to 110 TgN/yr by year 430. The largest N fixation increases were in the North Atlantic (factor of 4, with other basins between 1.5 and 2.0, auxiliary material Table S2). Arabian Sea N fixation increased by a factor of 2.3. Thus the strongest stabilizing feedback response was seen in the areas with the highest iron inputs from the atmosphere, where P initially limited N fixation. By year 430, P was still limiting in the

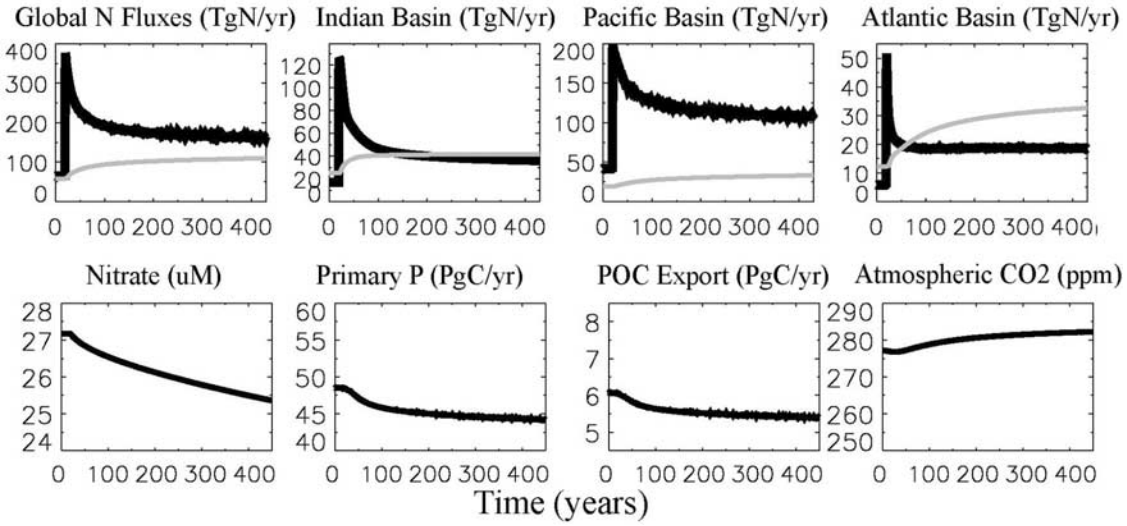

Figure 2. Global and basin-scale rates of N fixation (thin line) and denitrification (thick line) and selected global fluxes from the 430 year Case 1 experiment. In each plot the last 20 years of the control are plotted prior to the Case 1 simulation.

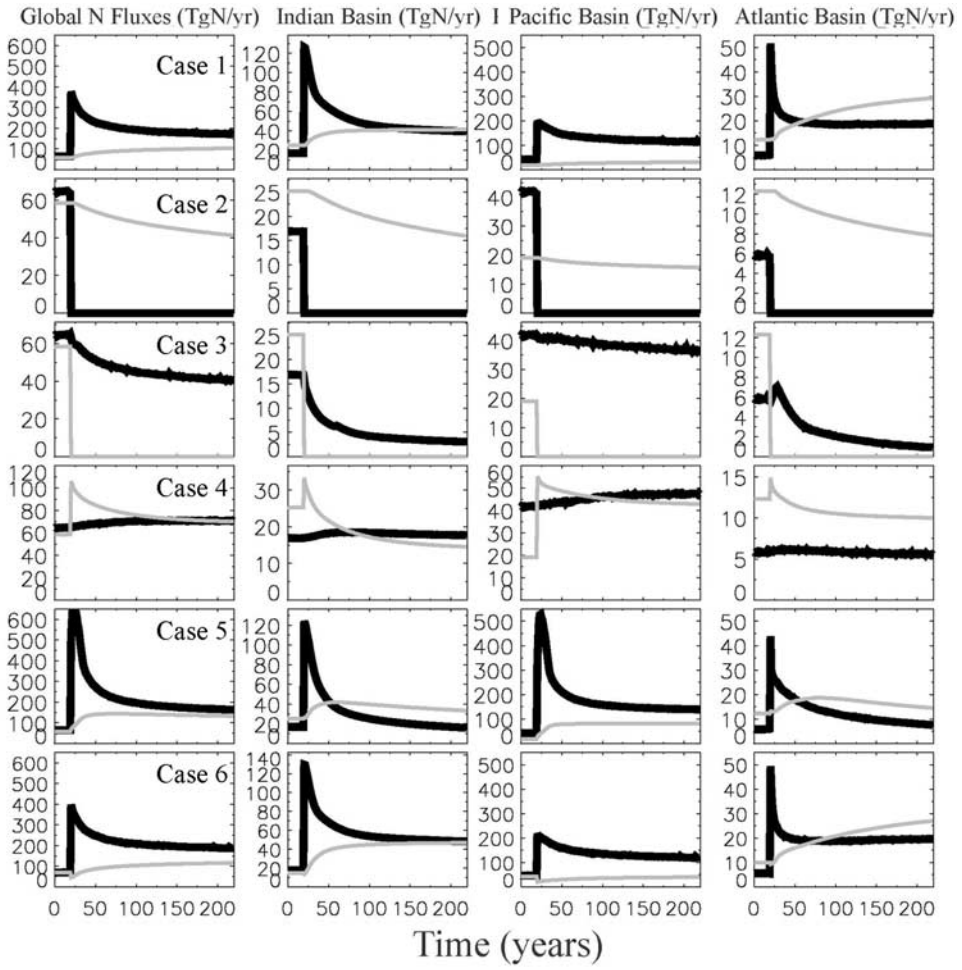

Figure 3. Global and basin-scale rates of N fixation (thin line) and denitrification (thick line) from each experiment are shown. Only the first 200 years of Case 1 are plotted for comparison with the other experiments. The last 20 years of the control are also shown in each plot.

N. Atlantic, but the N. Indian Ocean was limited by Fe or light. The largest increases in denitrification were in the S. Pacific (factor 3.5) and the S. Atlantic (factor 3.1). The eastern Pacific still dominated denitrification (66%, Indian 22%, and 11% Atlantic). The source-sink imbalance leads to a reduction in global fixed N inventory by 6.7% during the simulation. As N is depleted, it becomes more limiting for nondiazotroph growth rates reducing primary production (−9%), and export (−11%). This weakening of the biological pump led to an increased flux of CO_2 to the atmosphere, raising atmospheric CO_2 concentrations by 5.4 ppm (Figure 2 and auxiliary material Table S2).

[19] There were strong regional to basin-scale differences in the N-cycle response to perturbation (Figure 2). In the Indian Ocean, N fixation increases rapidly during the first ~30 years of the simulation, roughly balancing basin denitrification after 100 years. A similar, but more gradual increase in N fixation is seen in the Atlantic. The different timescales arise because areas of N fixation and denitrification are essentially colocated in the Indian, while low N/P waters take time to be advected to N fixation regions in the Atlantic. By the end of the simulation, Atlantic N fixation is 14 TgN/yr higher than denitrification and still rising (Figure 2). The N fixation feedback response in the Pacific is weaker than in the other basins, increasing by factors of 1.8 and 1.7 for the north and south Pacific respectively. The south Indian Ocean had an even weaker response, increasing by a factor of 1.5 (auxiliary material Table S2). In these regions, the diazotrophs are limited by iron availability, and thus are less sensitive to variations in surface water N/P ratios. Interestingly though, there is still an advantage conferred as the other phytoplankton become increasingly more N stressed, allowing the diazotrophs to compete more effectively for the available Fe, increasing N fixation.

[20] In Case 2 (no denitrification), N fixation declined steadily from 58 to 41 TgN/yr, as surface water N/P ratios increased (Figure 3). Global N inventory rose 1.8%, leading to increased primary and export production. The stronger biological pump decreased atmospheric CO_2 by 4 ppm (auxiliary material Figure S1 and Table S2). The N fixation response to changes in denitrification was stronger in the

Atlantic and Indian (37% decrease in both) than in the Pacific (18% decrease).

[21] In Case 3 (no N fixation), denitrification declined rapidly in the Indian and Atlantic basins, falling to rates that were only 18% and 16% of the Control (Figure 3 and auxiliary material Table S2). The export of organic matter fueled by N fixation appears critical for maintaining low O_2 and denitrification in these regions. *Brandes et al.* [1998] estimated that 30–40% of the nitrate fueling export in the Arabian Sea comes from N fixation based on isotopic constraints. A strong on/off sensitivity to organic flux was suggested by *Suthof et al.* [2001]. In contrast, denitrification in the Pacific is less affected by N fixation (declining by 13%) (Figure 3 and auxiliary material Table S2). In this region, simulated export is driven by upwelling with less influence by N fixation. Nitrogen inventory declines by 1.7% decreasing primary and export production and increasing atmospheric CO_2 by 8 ppm (auxiliary material Figure S1 and Table S2).

[22] In Case 4 (lower diazotroph optimal Fe quota and Fe uptake half-saturation constant), N fixation rose initially to 106 TgN/yr then declined to ~70 TgN/yr after 100 years (Figure 3). The strongest increase was in the Fe-limited Pacific basin, where at year 200 N fixation rates were more than double Control values. This basin remained Fe-limited for diazotrophs (even with lower quota and Ks values) throughout the experiment. By contrast, the Atlantic and Indian oceans are strongly P limited by the end of the experiment, and the initial burst of elevated N fixation collapsed resulting in lower N fixation levels than prior to the perturbation. N inventory increased slightly during the experiment, and there was increased primary and export production, decreasing atmospheric CO_2 (−5 ppm, auxiliary material Table S2 and Figure S1). Denitrification increased only slightly in each basin, owing to the artificial nitrate constraint.

[23] In Cases 1–3, the negative feedbacks operated least efficiently in the Pacific, where diazotrophs were Fe limited. There was a large increase in Pacific N fixation in response to decreased Fe stress (Case 4). To further test the role of Fe as a limiting factor, we conducted a simulation (Case 5) identical to Case 1, except the oceans were forced with the higher LGM dust inputs [*Mahowald et al.*, 2006]. Globally the gap between denitrification and N fixation narrowed much more rapidly in this simulation following the initial perturbation, ending with a net N loss of 30 TgN/yr (Case 1 was 70 TgN/yr, auxiliary material Table S2 and Figure 3). N fixation exceeded denitrification in the Indian and Atlantic, while the gap in the Pacific narrowed considerably (Figure 3). N fixation increasing by a factor of 5.2 in the S. Pacific and 3.8 in the N. Pacific relative to the control, while denitrification also increased by a factor of 3.3 (auxiliary material Table S2). Increased iron inputs increased production and export by diatoms as seen previously [*Moore et al.*, 2004, 2006], leading to more efficient export and less surface recycling, decreasing primary production. This community shift along with increased N fixation drives increased export and a drawdown of atmospheric CO_2 of −16 ppm (auxiliary material Figure S1 and Table S2).

[24] Strong Pacific Fe limitation of diazotrophs was critical to our results. It is possible that other diazotrophs are more efficient in Fe uptake or utilization than our model diazotrophs (based on *Trichodesmium*). Case 6 tested whether this would alter our conclusions by setting diazotroph Fe quotas and uptake parameters to those of our small phytoplankton group values, an extreme lower bound as Fe requirements are higher for diazotrophs [*Kustka et al.*, 2003b]. The Pacific basin N fixation increase is larger in Case 6 than Case 1, but the gap between N fixation and denitrification is actually larger still as denitrification increases as well (Figure 3 and auxiliary material Table S2). Fe remains limiting throughout the Pacific.

[25] The balance between N fixation and denitrification in conjunction with ocean circulation determine the surface water N/P ratio that can influence phytoplankton community structure, the strength of the biological pump and air-sea CO_2 flux. We examine the basin mean N* (= ($[NO_3^-]$ + $[NH_4^+]$) − 16 * $[PO_4^-]$) values in subeuphotic zone source waters (103–215 m) (auxiliary material Figure S2). In Cases 1 and 5, there was an initial sharp decrease in Pacific and Indian N* values due to high rates of denitrification. In Cases 1 and 6, Indian N* values reach ~−15 μM after 50 years then decline gradually, while the Pacific steadily declines over the simulations. Recall that in the Indian basin N fixation increases rapidly during the first few decades, approximately equal to denitrification after ~50 years (Figure 3). The more gradual, steady decrease in Atlantic N* values was consistent with advection of low N* waters from elsewhere and slowly increasing N fixation (Figure 3 and auxiliary material Figure S2). In the more Fe-replete Case 5, N* values in all three basins gradually increased after a rapid initial decrease.

[26] The spatial patterns of N fixation and denitrification illustrate key processes (Figure 4). Comparing Cases 1 and 5, higher dust inputs increased N fixation throughout the Pacific. The higher Fe inputs and N fixation increased export production in the eastern tropical Pacific, increasing denitrification rates (Case 5, Figure 4 and auxiliary material Table S2). The relaxation of Fe stress through parameter changes also increased Pacific N fixation (Cases 4 and 6). The decreased N fixation in Case 2 (no denitrification) is dramatic in the northern Indian Ocean. Similarly, in Case 3 (no N fixation) Indian denitrification is sharply decreased, highlighting close coupling in this region (Figures 3 and 4).

[27] We compared water column minimum dissolved O_2 concentrations from the World Ocean Atlas 2001 [*Conkright et al.*, 2002] (one degree data averaged onto our ocean grid) with our simulations (auxiliary material Figure S3). The WOA2001 observational climatology tends to overpredict O_2 concentrations in the core OMZs because of the averaging methods. A common problem with coarse resolution general circulation models is the tendency to upwell excessive amounts of nutrients in the eastern tropical Pacific [*Gnanadesikan et al.*, 2002; *Doney et al.*, 2004]. This contributes to the high rates of denitrification and a merging of the north and south OMZs. In the WOA2001 data the northward spread of low O_2 waters across the North Pacific is apparent, while these waters tend to remain more trapped in the eastern tropical Pacific in our simulations owing to

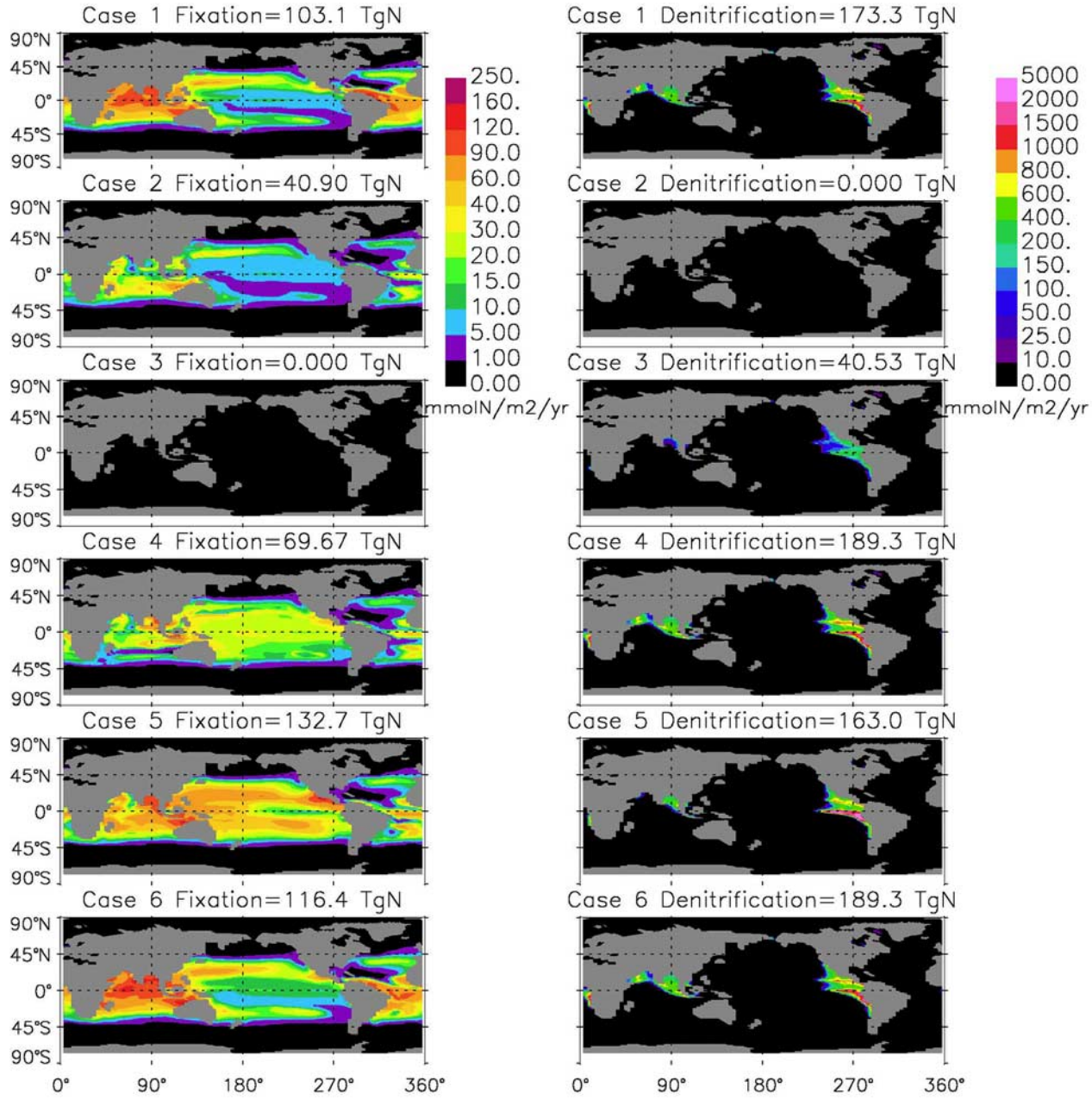

Figure 4. Spatial patterns of N fixation and denitrification are shown from year 200 of each simulation.

insufficient ventilation (auxiliary material Figure S3). Low O_2 concentrations are seen in the South Atlantic along the African coast in WOA2001 and our simulations. The OMZs decrease dramatically in the Indian and Atlantic basins without N fixation (Case 3, auxiliary material Figure S3). The rise in O_2 led to a near shutdown of denitrification (Figure 3 and auxiliary material Table S2).

[28] We computed the N* tracer (= ($[NO_3^-]$ + $[NH_4^+]$ − 16$[PO_4^-]$) for the WOA2001 gridded one-degree data averaging over depth ranges of 103–686 m (Figure 5) and the euphotic zone (<103 m, auxiliary material Figure S4). The WOA2001 data show positive values in the North Atlantic noted previously [*Michaels et al.*, 1996; *Gruber and Sarmiento*, 1997; *Mahaffey et al.*, 2005]. The highest simulated N* values are seen in this region, but values are still slightly negative at thermocline depths (Figure 5, but positive at the surface in auxiliary material Figure S4). In the south Atlantic, negative values are seen nearly everywhere in the WOA2001 data, with lowest values along the African coast. In the Pacific the WOA2001 data are strongly negative in the eastern tropics north and south of the equator, with less negative to positive values at midlatitudes on the western side of the basin, as noted by *Deutsch et al.* [2001].

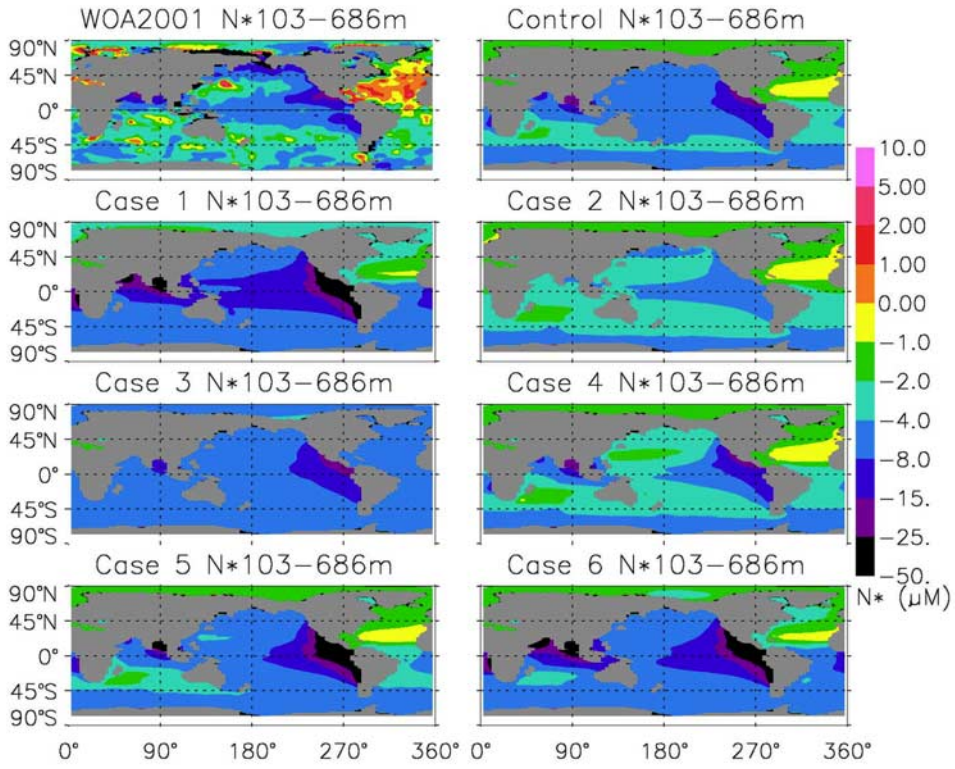

Figure 5. N* tracer (see text) averaged over the depth range 103–686 m plotted from the World Ocean Atlas 2001 data [*Conkright et al.*, 2002], from our control (year 2050), and from case experiment simulations (year 200).

[29] In the control simulation, N* values tend to be higher than the observations in each of the main OMZ regions, particularly the Arabian Sea. This suggests that denitrification is underestimated, not surprising given the artificial constraint and lack of sedimentary denitrification. In Case 1 N* values were considerably lower in the OMZs and adjacent regions than in WOA2001. Cases 2–4 illustrate how quickly global scale patterns of N* can change with variations in denitrification and N fixation. The regions of very low N* are smaller in Case 5 than in Case 1 owing to both increased N fixation and decreased denitrification, but these areas are still larger in extent and more negative than in WOA2001 (Figure 5). WOA2001 N* values in the Arctic are generally lower than in our simulations perhaps driven by sedimentary denitrification across the broad shelf regions. Case 4 resulted in surface N* values much higher than WOA2001 everywhere owing to elevated N fixation but constrained denitrification (auxiliary material Figure S4).

[30] Auxiliary material Figures S3 and S4 and Figure 5 can help evaluate our simulations. Oxygen concentrations and N* values are well below observations in the tropical eastern Pacific for Cases 1, 5, and 6, likely indicating denitrification is overestimated in this region. Observation-based estimates for water column denitrification here are typically ~40–50 TgN/yr [*Codispoti and Richards*, 1976; *Codispoti and Packard*, 1980; *Codispoti*, 1989; *Deutsch et al.*, 2001], much lower than in Cases 1, 5, and 6 (>100 TgN/yr, auxiliary material Table S2). Similarly, oxygen and N* values are considerably lower than observations in the Bay of Bengal and adjacent regions, with denitrification likely significantly overestimated. *Howell et al.* [1997] found little evidence for active water column denitrification during the 1995 northeast monsoon. In the Arabian Sea most recent estimates for water column denitrification are ~20–30 TgN/yr [*Naqvi*, 1987; *Naqvi and Shailaja*, 1993; *Howell et al.*, 1997; *Bange et al.*, 2000]. Our last year simulated Arabian Sea denitrification was 17 TgN/yr for Case 1 and <6 TgN/yr otherwise. Surface N* distributions are in reasonable agreement with WOA2001 in the Atlantic and Indian basins, but low relative to observations in the Pacific for Cases 1 and 6 (auxiliary material Figure S4). Low Pacific values reflect the very low N* in subsurface waters (auxiliary material Figure S2 and Figure 5) and may also indicate that N fixation is underestimated in this region.

4. Discussion

[31] Across our simulations there is substantial evidence for N inventory stabilizing feedbacks. In all cases, anomalies in denitrification rates were positively correlated with anomalies in N fixation. In the northern Indian ocean, in particular, there was a close coupling with response timescales of a few of decades. The Atlantic also responded with

stabilizing feedbacks but over centennial timescales. This reflects the time for advection of low N/P waters from other regions to the Atlantic (partly through the Arctic [*Yamamoto-Kawai et al.*, 2006]). At the end of Case 1, Atlantic N fixation continued to drift upward, driven by a N deficit generated mainly in the Pacific (Figure 2 and auxiliary material Figure S2). Significant portions of the Atlantic and Indian basins were P-limited for the diazotrophs, giving N fixation a strong sensitivity to N/P ratios in surface waters and a strong feedback response, a relationship assumed to hold globally in previous studies [*Tyrrell*, 1999; *Lenton and Watson*, 2000]. The Pacific stood out as an area where the stabilizing feedbacks were muted, driven by diazotroph Fe limitation that led to a spatial separation between the zones of N fixation and denitrification. Thus N fixation had a modest impact on the organic flux sinking into the OMZs, and changes in the N/P ratios in surface waters had a weaker impact on N fixation. Our results in this region are robust to even drastic changes in the iron-related diazotroph parameters (Cases 4 and 6).

[32] Our simulations had elevated N fixation along the northern edge of the HNLC zone in the eastern equatorial Pacific, driven by dust inputs from North America. This is the region where *Sigman et al.* [2005] suggested the possibility of high N fixation rates, off the Baja peninsula, based on nitrate N and O isotopic values. Our results are consistent, with higher N fixation there, but suggest that farther south the diazotrophs would be more Fe stressed and the linkage between denitrification and N fixation would be weaker.

[33] Our results differ from *Deutsch et al.*'s [2007] estimates of high N fixation rates within the upwelling zone and maximum rates to the south of the HNLC region. They suggest a minimal role for Fe limitation and a close coupling between N fixation and denitrification. Their results are diagnosed from observed nutrient and model circulation fields. In their sensitivity studies, altered circulation, observational nutrient errors, and DOM assumptions could move much of this tropical N fixation to the subtropics, but with little effect on basin total N fixation. Further, the coarse resolution model they used may overestimate upwelling nutrient flux [*Gnanadesikan et al.*, 2002; *Doney et al.*, 2004], with low N/P ratios (high excess P) which would lead to overestimation of N fixation as nutrients are forced back to observed concentrations. *Trichodesmium* sharply reduces N fixation when nitrate is available [*Holl and Montoya*, 2005] as in the equatorial Pacific. Thus high N fixation rates within the upwelling zone seems unlikely. Our Pacific N fixation was much lower than their estimate of 95 TgN/yr, ranging from 33 to 43 TgN/yr (Cases 1, 4, and 6) to a high value of 82 TgN/yr with the LGM dust flux; other recent estimates include 59 TgN/yr [*Deutsch et al.*, 2001] and 48–59 TgN/yr [*Galloway et al.*, 2004]. Future fieldwork will have to address the key question surrounding the extent of Fe limitation of N fixation in the tropical and subtropical Pacific.

[34] While much of our focus is on the centennial timescale feedbacks between denitrification and N fixation, each process also exhibited strong self-limiting feedbacks, independent of each other in our simulations. In Case 4, the initial peak in N fixation declined as P and Fe were depleted in the surface ocean. Cases 1, 5 and 6 all had initial sharp increases in denitrification that declined rapidly within the first few decades, much of this early decrease was due to the reduction in upwelled N, which in turn decreased the export flux of organic matter into portions of the OMZs.

[35] It seems unlikely that the widespread N limitation in the oceans today arises solely from interactions between diazotrophs and other phytoplankton in the context of inorganic N/P ratios [*Tyrrell*, 1999; *Lenton and Watson*, 2000]. If these interactions did lead to N being the proximate nutrient in surface waters, then one would expect freshwater systems to also be N limited, as N adjusted to P inputs. However, limnological systems tend to be P limited with diazotrophs making up any N deficits, suggesting that some factor, perhaps iron, unrelated to N/P ratios must prevent N fixation from providing balance to P in the oceans [*Vitousek and Howarth*, 1991]. We suggest Fe is the ultimate limiting nutrient leading to N being the proximate nutrient over wide regions today. Combined with the direct control of Fe in the High Nutrient, Low Chlorophyll (HNLC) regions, this suggests a dominant control of Fe on marine productivity and export globally [*Fung et al.*, 2000] with strong sensitivity to variations in atmospheric dust deposition [*Moore et al.*, 2006]. Several recent studies have noted the potential feedbacks between dust, ocean biogeochemistry and climate [*Michaels et al.*, 2001; *Karl et al.*, 2002; *Gruber*, 2004; *Moore et al.*, 2004, 2006; *Parekh et al.*, 2006]. *Tyrrell* [1999] and *Lenton and Watson* [2000] both noted the potentially complicating influence of Fe on N fixation. Other forcings such as the mixing-irradiance regime and sea surface temperatures could also impact N fixation in the context of climate change [*Boyd and Doney*, 2002]. It is not valid to infer N fixation rates on the basis of the N/P balance in surface waters alone. High rates of N fixation are observed in the North Atlantic, a region with positive N* [*Capone et al.*, 2005], and relatively low N fixation rates were predicted in our simulations for the Pacific basin, which had the lowest values of N*.

[36] Our results illustrate some interesting links between N inventory and climate. The N inventory perturbations impacted the strength of the biological pump and air-sea CO_2 flux, modifying atmospheric CO_2 concentrations by a range of +8 to −16 ppm over centennial timescales (Figure 2 and auxiliary material Figure S1 and Table S2; the range would be +10.7 to −13.7 ppm accounting for the control drift). These changes in atmospheric CO_2 are somewhat larger than estimates of pre-industrial Holocene centennial timescale atmospheric CO_2 variations based on coupled carbon-climate simulations [*Doney et al.*, 2006] and high-deposition ice cores [*Siegenthaler et al.*, 2005]. This corroborates *Gruber and Sarmiento*'s [1997] finding that marine N cycle imbalances as large as those simulated here have not persisted for more than a few hundred years in recent times. We did induce very strong, likely unrealistic perturbations. Alternatively, it is also possible that negative feedbacks operate more efficiently in the real ocean than in our model. Iron uptake efficiency and quotas for *Trichodesmium spp*. are relatively well known [i.e., *Berman-Frank et al.*, 2001]. Little is known about other

diazotrophs, including their quantitative importance in global N fixation. Our simulations, therefore, may overestimate the impact of Fe availability on N fixation. However, our conclusions are not overly sensitive to chosen diazotroph Fe parameters (Case 6). Possibly N cycle imbalance is a recent phenomenon. Greenhouse gas induced climate change may be acting to slow O_2 ventilation rates, increasing denitrification [*Meissner et al.*, 2005]. Dust deposition may be decreasing as rising atmospheric CO_2 fuels increased vegetative cover in arid regions [*Mahowald et al.*, 2006], leading to increased Fe stress of the diazotrophs, depressing N fixation. This effect may have already reduced N fixation by ~18% since pre-industrial times [*Moore et al.*, 2006].

[37] It is critical to consider the three dimensional context of the marine N cycle when examining climate impacts. The Case 1 and 5 experiments both lost similar amounts of N globally (4.1% and 3.5% over 200 years), but this loss was more concentrated near the surface in Case 1 leading to a weakened biological pump and an increase in atmospheric CO_2 (+4 ppm). In contrast, the large increases in N fixation and atmospheric Fe inputs in Case 5 strengthened the biological pump leading to a decrease in atmospheric CO_2 (−16 ppm, auxiliary material Table S2). Both simulations lost fixed N, but had opposite impacts on climate (at least on centennial timescales). The location (i.e., shallow subsurface versus middepths, coastal versus deep ocean sediments) of perturbations in denitrification rates in conjunction with ocean circulation and ventilation rates will determine the timescale of this signal reaching surface waters and potentially impacting N fixation, the biological pump, and climate.

[38] Our results suggest that widespread Fe limitation limits the ability of N fixation to balance denitrification [*Falkowski*, 1997]. The strength of the stabilizing feedbacks was strongest in Case 4 with the LGM dust/iron inputs. The N imbalance at year 200 had the oceans losing 30 TgN/yr and closing, while for Case 1 the imbalance was −70 TgN/yr at year 200, and had decreased only to −51 TgN/yr by year 430 (see also auxiliary materials for more discussion of feedback strengths). Owing to widespread diazotroph Fe limitation, export production and air-sea CO_2 flux are sensitive to climate driven variations in mineral dust deposition at mid to low latitudes, even outside the HNLC regions [*Michaels et al.*, 2001; *Moore et al.*, 2006]. The biogeochemical impact of dust variations on C export and air-sea CO_2 flux due to this indirect dust–N fixation–carbon pathway can rival the more direct impacts in the HNLC regions [*Moore et al.*, 2006]. In the glacial climate with increased Fe inputs from dust deposition, N fixation would adjust more efficiently to balance denitrification, likely erasing the N deficit observed in the modern ocean. This would strengthen the biological pump, accounting for some of the observed glacial decreases in atmospheric CO_2 [*Falkowski*, 1997] and the postglacial rise in atmospheric CO_2 as the N deficit was generated [*Broecker and Henderson*, 1998]. Both N fixation and denitrification global rates may actually have been lower in the glacial period [*Christensen*, 1994; *Altabet et al.*, 1995; *Ganeshram et al.*, 1995, 2002; *Meissner et al.*, 2005]. However, a better balance between sources and sinks would have pushed the oceans from the current strong N deficit to a more balanced system, perhaps even a positive N*, P-limited ocean as seen in the North Atlantic today. *Deutsch et al.* [2004] argued that N inventory could not have increased by more than 30% in glacial times with an increase of at most 10% more likely based on N isotope records and constraints. However, even a 10% inventory increase would largely wipe out the current N deficit and have a significant impact on atmospheric CO_2.

[39] **Acknowledgments.** The authors would like to thank Curtis Deutsch and Nick Stephens for helpful reviews of this manuscript. This work was supported by grants from the U.S. National Science Foundation (OCE-0222033 and OCE-0452972). Computations supported by Earth System Modeling Facility (NSF ATM-0321380) and by the Climate Simulation Laboratory at the National Center for Atmospheric Research. The National Center for Atmospheric Research is sponsored by the U.S. National Science Foundation.

References

Altabet, M. A., M. J. Higginson, D. W. Murray, and W. L. Prell (1995), Climate-related variations in denitrification in the Arabian Sea from sediment 15N/14N ratios, *Nature*, *373*, 506–509.

Altabet, M. A., M. J. Higginson, and D. W. Murray (2002), The effect of millenial-scale changes in Arabian Sea denitrification on atmospheric CO_2, *Nature*, *415*, 159–162.

Ammerman, J. W., R. R. Hood, D. A. Case, and J. B. Cotner (2003), Phosphorus deficiency in the Atlantic: An emerging paradigm in oceanography, *Eos Trans. AGU*, *84*(18), 165.

Bange, H. W., T. Rixen, A. M. Johansen, R. L. Siefert, R. Ramesh, V. Ittekkot, M. R. Hoffman, and M. O. Andreae (2000), A revised nitrogen budget for the Arabian Sea, *Global Biogeochem. Cycles*, *14*(4), 1283–1297.

Bange, H. W., S. W. A. Naqvi, and L. A. Codispoti (2005), The nitrogen cycle in the Arabian Sea, *Prog. Oceanogr.*, *65*, 145–158.

Berman-Frank, I., J. T. Cullen, Y. Shaked, R. M. Sherrell, and P. G. Falkowski (2001), Iron availability, cellular iron quotas, and N fixation in *Trichodesmium*, *Limnol. Oceanogr.*, *46*, 1249–1260.

Boyd, P. W., and S. C. Doney (2002), Modelling regional responses by marine pelagic ecosystems to global climate change, *Geophys. Res. Lett.*, *29*(16), 1806, doi:10.1029/2001GL014130.

Brandes, J. A., and A. H. Devol (2002), A global marine-fixed nitrogen isotopic budget: Implications for Holocene nitrogen cycling, *Global Biogeochem. Cycles*, *16*(4), 1120, doi:10.1029/2001GB001856.

Brandes, J. A., A. H. Devol, T. Yoshinari, D. A. Jayakumar, and S. W. A. Naqvi (1998), Isotopic composition of nitrate in the central Arabian Sea and eastern tropical North Pacific: A tracer for mixing and nitrogen cycles, *Limnol. Oceanogr.*, *43*, 1680–1689.

Broecker, W. S., and G. M. Henderson (1998), The sequence of events surrounding Termination II and their implications for the cause of glacial-interglacial CO_2 changes, *Paleoceanography*, *13*(4), 352–364.

Calvert, S. E., and N. B. Price (1971), Upwelling and nutrient regeneration in the Benguela Current, October, 1968, *Deep Sea Res.*, *18*, 505–523.

Capone, D. G., J. P. Zehr, H. W. Paerl, B. Bergman, and E. J. Carpenter (1997), *Trichodesmium*, a globally significant marine cyanobacterium, *Science*, *275*, 1221–1229.

Capone, D. G., J. A. Burns, J. P. Montoya, A. Subramaniam, C. Mahaffey, T. Gunderson, A. F. Michaels, and E. J. Carpenter (2005), N fixation by *Trichodesmium* spp.: An important source of new nitrogen to the tropical and subtropical North Atlantic Ocean, *Global Biogeochem. Cycles*, *19*, GB2024, doi:10.1029/2004GB002331.

Christensen, J. P. (1994), Carbon export from continental shelves, denitrification and atmospheric carbon dioxide, *Cont. Shelf Res.*, *14*(5), 547–576.

Codispoti, L. A. (1989), Phosphorus vs. nitrogen limitation of new and export production, in *Productivity of the Oceans, Past and Present*, edited by W. H. Berger, V. S. Smetacek, and G. Wefer, pp. 377–394, John Wiley, Hoboken, N. J.

Codispoti, L. A., and J. P. Christensen (1985), Nitrification, denitrification, and nitrous oxide cycling in the eastern tropical south Pacific Ocean, *Mar. Chem.*, *16*, 277–300.

Codispoti, L. A., and T. T. Packard (1980), Denitrification rates in the eastern tropical South Pacific, *J. Mar. Res.*, *38*, 453–477.

Codispoti, L. A., and F. A. Richards (1976), An analysis of the horizontal regime of denitrification in the eastern tropical North Pacific, *Limnol. Oceanogr.*, *21*, 379–388.

Codispoti, L. A., J. A. Brandes, J. P. Christensen, A. H. Devol, S. W. A. Naqvi, H. W. Paerl, and T. Yoshinari (2001), The oceanic fixed nitrogen and nitrous oxide budgets: Moving targets as we enter the anthropocene?, *Sci. Mar.*, *65*, Suppl., 85–105.

Collins, W. D., et al. (2006), The Community Climate System Model: CCSM3, *J. Clim.*, *19*, 2122–2143.

Conkright, M. E., et al. (1998), World Ocean Database 1998 CD-ROM data set documentation, *Internal Rep. 14*, Natl. Oceanogr. Data Cent., Silver Spring, Md.

Conkright, M. E., R. A. Locarnini, H. E. Garcia, T. D. O'Brien, T. P. Boyer, C. Stevens, and J. I. Antonov (2002), *World Ocean Atlas 2001: Objective Analysis, Data Statistics, and Figures* [CD-ROM], Natl. Oceanogr. Data Cent., Silver Spring, Md.

Davis, C. S., and D. J. McGillicuddy Jr. (2006), Transatlantic abundance of the N_2-fixing colonial cyanobacterium *Trichodesmium*, *Science*, *312*, 1517, doi:10.1126/science.1123570.

Deutsch, C., N. Gruber, R. M. Key, J. L. Sarmiento, and A. Ganachaud (2001), Denitrification and N_2 fixation in the Pacific Ocean, *Global Biogeochem. Cycles*, *15*(2), 483–506.

Deutsch, C., D. M. Sigman, R. C. Thunell, A. N. Meckler, and G. H. Haug (2004), Isotopic constraints on glacial/interglacial changes in the oceanic nitrogen budget, *Global Biogeochem. Cycles*, *18*, GB4012, doi:10.1029/2003GB002189.

Deutsch, C., J. L. Sarmiento, D. M. Sigman, N. Gruber, and J. P. Dunne (2007), Spatial coupling of nitrogen inputs and losses in the ocean, *Nature*, *445*, doi:10.1038/nature05392.

Doney, S. C., K. Lindsay, and J. K. Moore (2003), Global ocean carbon cycle modeling, in *Ocean Biogeochemistry*, edited by M. Fasham, pp. 217–238, Springer, New York.

Doney, S. C., et al. (2004), Evaluating global ocean carbon models: The importance of realistic physics, *Global Biogeochem. Cycles*, *18*, GB3017, doi:10.1029/2003GB002150.

Doney, S. C., K. Lindsay, I. Fung, and J. John (2006), Natural variability in a stable 2000 year coupled climate-carbon cycle simulation, *J. Clim.*, *19*, 3033–3054.

Dugdale, R. C., and F. P. Wilkerson (1998), Silicate regulation of new production in the equatorial Pacific upwelling, *Nature*, *391*, 270–273.

Dyhrman, S. T., E. A. Webb, A. Anderson, D. M. Moffett, and J. B. Waterbury (2002), Cell-specific detection of phosphorus stress in *Trichodesmium* from the western North Atlantic, *Limnol. Oceanogr.*, *47*, 1832–1836.

Dyhrman, S. T., P. D. Chappell, S. T. Haley, J. W. Moffett, E. D. Orchard, J. B. Waterbury, and E. A. Webb (2006), Phosphonate utilization by the globally important marine diazotroph *Trichodesmium*, *Nature*, *439*, 68–71, doi:10.1038/nature04203.

Falkowski, P. G. (1997), Evolution of the nitrogen cycle and its influence on the biological sequestration of CO_2 in the ocean, *Nature*, *387*, 272–275.

Fung, I. Y., S. K. Meyn, I. Tegen, S. C. Doney, J. G. John, and J. K. B. Bishop (2000), Iron supply and demand in the upper ocean, *Global Biogeochem. Cycles*, *14*(1), 281–295.

Galloway, J. N., et al. (2004), Nitrogen cycles: Past, present, and future, *Biogeochemistry*, *70*, 153–226.

Ganeshram, R. S., T. F. Pedersen, S. E. Calvert, and J. W. Murray (1995), Large changes in oceanic nutrient inventories from glacial to interglacial periods, *Nature*, *376*, 755–758.

Ganeshram, R. S., T. F. Pedersen, S. E. Calvert, and R. Francois (2002), Reduced N fixation in the glacial ocean inferred from changes in marine nitrogen and phosphorus inventories, *Nature*, *415*, 156–159.

Gnanadesikan, A., R. D. Slater, N. Gruber, and J. L. Sarmiento (2002), Oceanic vertical exchange and new production: A comparison between models and observations, *Deep Sea Res., Part II*, *49*, 363–401.

Gruber, N. (2004), The dynamics of the marine nitrogen cycle and its influence on atmospheric CO_2 variations, in *The Ocean Carbon Cycle*, edited by M. Follows and T. Oguz, pp. 97–148, Springer, New York.

Gruber, N., and J. L. Sarmiento (1997), Global patterns of marine N fixation and denitrification, *Global Biogeochem. Cycles*, *11*(2), 235–266.

Hansell, D. A., N. R. Bates, and D. B. Olson (2004), Excess nitrate and N fixation in the North Atlantic Ocean, *Mar. Chem.*, *84*, 243–265.

Holl, C. M., and J. P. Montoya (2005), Interactions between nitrate uptake and nitrogen fixation in continuous cultures of the marine diazotroph *Trichodesmium* (cyanobacteria), *J. Phycol.*, *41*(6), 1178–1183.

Howell, E. A., S. C. Doney, R. A. Fine, and D. B. Olson (1997), Geochemical estimates of denitrification in the Arabian Sea and the Bay of Bengal during WOCE, *Geophys. Res. Lett.*, *24*(21), 2549–2552.

Karl, D., A. Michaels, B. Bergman, D. Capone, E. Carpenter, R. Letelier, F. Lipschultz, H. Paerl, D. Sigman, and L. Stal (2002), DiN fixation in the world's oceans, *Biogeochemistry*, *57/58*, 47–98.

Key, R. M., A. Kozyr, C. L. Sabine, K. Lee, R. Wanninkhof, J. L. Bullister, R. A. Feely, F. J. Millero, C. Mordy, and T.-H. Peng (2004), A global ocean carbon climatology: Results from Global Data Analysis Project (GLODAP), *Global Biogeochem. Cycles*, *18*, GB4031, doi:10.1029/2004GB002247.

Kustka, A., S. Sañudo-Wilhelmy, E. J. Carpenter, D. G. Capone, J. Burns, and W. G. Sunda (2003a), Iron requirements for nitrogen- and ammonium-supported growth in cultures of *Trichodesmium* (IMS101): Comparison with N fixation rates and iron:carbon ratios of field populations, *Limnol. Oceanogr.*, *48*, 1869–1884.

Kustka, A., S. Sañudo-Wilhelmy, E. J. Carpenter, D. G. Capone, and J. A. Raven (2003b), A revised estimate of the iron use efficiency of N fixation, with special reference to the marine cyanobacterium *Trichodesmium SPP.* (CYANOPHYTA), *J. Phycol.*, *39*, 12–25.

Large, W. G. and S. G. Yeager (2004), Diurnal to decadal global forcing for ocean and sea-ice models: The data sets and flux climatologies. *NCAR Tech. Note NCAR/TN-460+STR*, 111 pp., Natl. Cent. for Atmos. Res., Boulder, Colo.

Lee, K., D. M. Karl, R. Wanninkhof, and J. Z. Zhang (2002), Global estimates of net carbon production in the nitrate-depleted tropical and subtropical oceans, *Geophys. Res. Lett.*, *29*(19), 1907, doi:10.1029/2001GL014198.

Lenton, T. M., and A. J. Watson (2000), Redfield revisited: 1. Regulation of nitrate, phosphate, and oxygen in the ocean, *Global Biogeochem. Cycles*, *14*(1), 225–248.

Luo, C., N. Mahowald, and J. del Corral (2003), Sensitivity study of meteorological parameters on mineral aerosol mobilization, transport and distribution, *J. Geophys. Res.*, *108*(D15), 4447, doi:10.1029/2003JD003483.

Mahaffey, C., A. F. Michaels, and D. G. Capone (2005), The conundrum of marine N_2 fixation, *Am. J. Sci.*, *305*, 546–595.

Mahowald, N. M., D. R. Muhs, S. Levis, P. J. Rasch, M. Yoshioka, C. S. Zender, and C. Luo (2006), Change in atmospheric mineral aerosols in response to climate: Last glacial period, preindustrial, modern, and doubled carbon dioxide climates, *J. Geophys. Res.*, *111*, D10202, doi:10.1029/2005JD006653.

Martin, J. H., R. M. Gordon, and S. E. Fitzwater (1991), The case for iron, *Limnol. Oceanogr.*, *36*, 1793–1802.

McElroy, M. B. (1983), Marine biological controls on atmospheric CO_2 and climate, *Nature*, *302*, 328–329.

Meissner, K. J., E. D. Galbraith, and C. Völker (2005), Denitrification under glacial and interglacial conditions: A physical approach, *Paleoceanography*, *20*, PA3001, doi:10.1029/2004PA001083.

Michaels, A. F., D. Olson, J. L. Sarmiento, J. W. Ammerman, K. Fanning, R. Jahnke, A. H. Knap, F. Lipschultz, and J. M. Prospero (1996), Inputs, losses and transformations of nitrogen and phosphorus in the pelagic North Atlantic Ocean, *Biogeochemistry*, *35*, 181–226.

Michaels, A. F., D. M. Karl, and D. G. Capone (2001), Elemental stoichiometry, new production, and N fixation, *Oceanography*, *14*(4), 68–77.

Middleburg, J. J., K. Soetaert, P. M. J. Herman, and C. H. R. Heip (1996), Denitrification in marine sediments: A model study, *Global Biogeochem. Cycles*, *10*(4), 661–673.

Mills, M. M., C. Ridame, M. Davey, J. La Roche, and R. J. Geider (2004), Iron and phosphorus co-limit N fixation in the eastern tropical North Atlantic, *Nature*, *429*, 292–294.

Montoya, J. P., C. M. Holl, J. P. Zehr, A. Hansen, T. A. Villareal, and D. G. Capone (2004), High rates of N_2 fixation by unicellular diazotrophs in the oligotrophic Pacific Ocean, *Nature*, *430*, 1027–1031.

Moore, J. K., S. C. Doney, J. C. Kleypas, D. M. Glover, and I. Y. Fung (2002a), An intermediate complexity marine ecosystem model for the global domain, *Deep Sea Res., Part II*, *49*, 403–462.

Moore, J. K., S. C. Doney, D. M. Glover, and I. Y. Fung (2002b), Iron cycling and nutrient limitation patterns in surface waters of the world ocean, *Deep Sea Res., Part II*, *49*, 463–508.

Moore, J. K., S. C. Doney, and K. Lindsay (2004), Upper ocean ecosystem dynamics and iron cycling in a global three-dimensional model, *Global Biogeochem. Cycles*, *18*, GB4028, doi:10.1029/2004GB002220.

Moore, J. K., S. C. Doney, K. Lindsay, N. Mahowald, and A. F. Michaels (2006), N fixation amplifies the ocean biogeochemical response to decadal timescale variations in mineral dust deposition, *Tellus, Ser. B*, *58*, 560–572.

Naqvi, S. W. A. (1987), Some aspects of the oxygen-deficient conditions and denitrification in the Arabian Sea, *J. Mar. Res.*, *45*, 1049–1072.

Naqvi, S. W. A., and M. S. Shailaja (1993), Activity of the respiratory electron transport system and respiration rates within the oxygen minimum layer of the Arabian Sea, *Deep Sea Res., Part II*, *40*, 687–695.

Olson, D. B., G. L. Hitchcock, R. A. Fine, and B. A. Warren (1993), Maintenance of the low-oxygen layer in the central Arabian Sea, *Deep Sea Res.*, *40*, 673–685.

Parekh, P., M. J. Follows, S. Dutkiewicz, and T. Ito (2006), Physical and biological regulation of the soft tissue carbon pump, *Paleoceanography*, *21*, PA3001, doi:10.1029/2005PA001258.

Perry, M. J., and R. W. Eppley (1981), Phosphate uptake by phytoplankton in the central North Pacific Ocean, *Deep Sea Res., Part A*, *28*, 39–49.

Redfield, A. C. (1958), The biological control of chemical factors in the environment, *Am. Sci.*, *46*, 204–221.

Ryther, J. H., and W. M. Dunstan (1971), Nitrogen, phosphorus, and eutrophication in the coastal marine environment, *Science*, *171*, 1008–1013.

Sañudo-Wilhelmy, S. A., A. B. Kustka, C. J. Gobler, D. A. Hutchins, M. Yang, K. Lwiza, J. Burns, D. G. Capone, J. A. Raven, and E. J. Carpenter (2001), Phosphorus limitation of N fixation by *Trichodesmium* in the central Atlantic Ocean, *Nature*, *411*, 66–69.

Siegenthaler, U., E. Monnin, K. Kawamura, R. Spahni, J. Schwander, B. Stauffer, T. F. Stocker, J.-M. Barnola, and H. Fisher (2005), Supporting evidence from the EPICA Dronning Maud Land ice core for atmospheric CO_2 changes during the past millennium, *Tellus, Ser. B*, *57*, 51–57.

Sigman, D. M., J. Granger, P. J. DiFiore, M. M. Lehmann, R. Ho, G. Cane, and A. van Geen (2005), Coupled nitrogen and oxygen isotope measurements of nitrate along the eastern North Pacific margin, *Global Biogeochem. Cycles*, *19*, GB4022, doi:10.1029/2005GB002458.

Sohm, J. A., and D. G. Capone (2007), Phosphorus dynamics of the tropical and subtropical North Atlantic: *Trichodesmium* vs. bulk plankton, *Mar. Ecol. Prog. Ser.*, in press.

Suthof, A., V. Ittekot, and B. Gaye-Haake (2001), Millenial-scale oscillation of denitrification in the Arabian Sea during the late Quaternary and its potential influence on atmospheric N_2O and global climate, *Global Biogeochem. Cycles*, *15*(3), 637–649.

Tyrrell, T. (1999), The relative influence of nitrogen and phosphorus on oceanic primary production, *Nature*, *400*, 525–531.

Tyrrell, T., and M. I. Lucas (2002), Geochemical evidence of denitrification in the Benguela upwelling system, *Cont. Shelf Res.*, *22*, 2497–2511.

Villareal, T. A. (1992), Marine nitrogen-fixing diatom-cyanobacteria symbioses, in *Marine Pelagic Cyanobacteria: Trichodesmium and other Diazotrophs*, edited by E. J. Carpenter et al., pp. 163–174, Springer, New York.

Vitousek, P. M., and R. W. Howarth (1991), Nitrogen limitation on land and in the sea: How can it occur?, *Biogeochemistry*, *13*, 87–115.

Wu, J., S. W. Chung, L. S. Wen, K. K. Liu, L. Chen, H. Y. Chen, and D. M. Karl (2003), Dissolved inorganic phosphorus, dissolved iron, and *Trichodesmium* in the oligotrophic South China Sea, *Global Biogeochem. Cycles*, *17*(1), 1008, doi:10.1029/2002GB001924.

Yamamoto-Kawai, M., E. Carmack, and F. McLaughlin (2006), Nitrogen balance and Arctic throughflow, *Nature*, *443*, 43.

Yeager, S. G., W. G. Large, J. J. Hack, and C. A. Shields (2004), The low resolution CCSM3, *J. Clim.*, *17*, 2545–2566.

Zehr, J. P., J. B. Waterbury, P. J. Turner, J. P. Montoya, E. Omoregie, G. F. Steward, A. Hansen, and D. M. Karl (2001), Unicellular cyanobacteria fix N_2 in the subtropical North Pacific Ocean, *Nature*, *412*, 635–638.

S. C. Doney, Department of Marine Chemistry and Geochemistry, Woods Hole Oceanographic Institution, MS 25 Woods Hole, MA 02543-1543, USA. (sdoney@whoi.edu)

J. K. Moore, Department of Earth System Science, University of California, Irvine, CA 92697-3100, USA. (jkmoore@uci.edu)

Auxiliary Methods

The BEC model was described by Moore et al. (2002; 2004). Here we review only some key aspects of the model relevant for the present study. The BEC model includes several phytoplankton functional groups including diatoms, calcifiers, diazotrophs, and picoplankton (Moore et al., 2002: 2004). The calcifiers are included implicitly as a variable fraction of our small phytoplankton group, according to environmental factors (Moore et al., 2004). These functional groups are believed to be important drivers of ocean biogeochemical cycles and are included specifically to promote the study of ocean biogeochemistry - climate interactions (Le Quéré et al., 2005; Hood et al., 2006). Our diazotroph functional group is parameterized largely based on observations of *Trichodesmium spp*. (Moore et al., 2002; 2004). To the extent that other diazotrophs may respond differently to environmental forcings, the model may not capture their dynamics well. Very little is known at present about how non-*Trichodesmium* species respond to environmental forcings. Several studies have modeled N fixation rates but did not include both Fe and P as potentially limiting factors (Hood et al., 2001; 2004; Fennel et al., 2002; Coles et al., 2004). We assume fixed C/N/P ratios for each phytoplankton group and for the sinking export of particulate organic matter (POM). These ratios are set close to the Redfield values (117C/16N/1P, Anderson and Sarmiento, 1994), with the exception of the diazotrophs that have an N/P ratio of 50 mol/mol, and the same C/N ratio as the other groups. We note that the N/P ratio of *Trichodesmium spp.* can vary considerably in different environments (Krauk et al., 2006), a feature not currently included in the model. Sinking particles are implicitly treated and assumed to sink and remineralize instantly within the water column at the same grid location where they are generated. The remineralization profiles are determined by a variant of the mineral ballast model proposed by Armstrong et al. (2002). In this model the sinking flux of mineral ballast (biogenic silica, calcium carbonate, and mineral dust particles) is presumed to transport some POM to the deep ocean which is remineralized with the same profiles as the ballast material (see Moore et al., 2004 for details). All nutrients are simulated globally over all depths with no restoring of any kind (Moore et al., 2004).

The parameter changes noted in Table S1 are similar to those described previously by Moore et al. (2006). The most significant effect is to increase iron scavenging in the deep ocean, while retaining similar rates in the upper ocean. The original iron related parameters worked well for the upper ocean but allowed the deep ocean to drift up to 0.6nM in most regions over longer simulations. Other changes make the diazotrophs somewhat more efficient at nutrient utilization. We have also modified the parameters associated with the remineralization profiles of soft POM and biogenic silica. These values gave a modestly better match to upper ocean observations of macronutrient concentrations.

Table S1. Parameter changes modified in this work relative to Moore et al. (2004).

Parameter	Original Value	Modified Value	Units
Ref_Particle	0.0066	0.002	nmolC/cm^2/s[A]
Fe_max_scale	4.0	3.0	unitless[B]
Fe_scav_threshold	0.4	0.5	nM Fe[C]
POC_fescav_scale	0.002	0.0	unitless[D]
diatom Kfe	0.16	0.15	nM Fe[E]
CaCO3_temp	5.0	1.0	^{o}C
alphaChl	0.25	0.3	nmolC/cm^2/ngChlWday[F]
alphaDiaz	0.03	0.036	nmolC/cm^2/ngChlWday[F]
diatom Knh4	0.008	0.08	μM N
diazotroph Kpo4	0.0075	0.005	μM P
diazotroph Kfe	0.1	0.09	nM Fe
diazotroph max Fe/C	48.0	42.0	μmolFe/molC
diazotroph N/P ratio	45.0	50.0	molN/molP
diazotroph mortality	0.18	0.16	per day
soft POM remin	42.0	130.0	m[G]
Q10 soft POM	2.0	1.12	unitless
soft bSi remin	32.0	22.0	m[H]
Q10 soft bSi	2.0	4.0	unitless
hard fraction bSi	0.55	0.37	unitless[I]
soft POM remin (where O2 < 4μM)		260.0	m[J]

A - reference particle flux used in calculating iron scavenging rates.
B - unitless maximum scaling factor of scavenging dependent on sinking particle flux.
C - threshold value below which iron scavenging rates are progressively decreased.
D - scaling factor for standing stock of particulate organic carbon used in Fe scavenging.
E - half saturation value for iron uptake by the diatoms.
F - initial slope of P vs. I curve, lower value for diazotrophs.
G - remineralization length scale for soft particulate organic matter.

H - remineralization length scale for soft biogenic silica.
I - fraction of bSi resistant to dissolution within water column.
J - remineralization length scale increased under low O_2 conditions based on Van Mooy et al., 2002.

Auxiliary Results and Discussion

There are very limited field observations of nitrogen fixation over seasonal timescales to compare our results with for model evaluation. Perhaps the best studied sites would be at the time series stations, BATS and HOT, where field estimates for N fixation are ~ 15 mmolN/m^2/yr at BATS (Orcutt et al., 2001) and range between ~31-51 mmolN/m^2/yr for HOT (Karl et al., 1997). We noted previously our low simulated values in the North Atlantic subtropical gyre. Our simulations are somewhat low at BATS due to extreme P limitation in this region ~ 3-6 mmolN/m^2/yr. At HOT our control simulation was rather low at 12 mmolN/m^2/yr (not surprising given the constraint on denitrification). For the simulations where the denitrification constraint was released we simulated values of 25, 74, and 37 mmolN/m^2/yr for cases 1, 5 (LGM dust), and 6, respectively during year 200. Table S2 summarizes the basin scale N fixation and denitrification in each of our experiments as well as the N cycle impacts on primary production, export production, and atmospheric CO_2 concentrations.

Our simulations can be compared with two other global scale estimates of N fixation. Lee et al. (2002) estimated N fixation based on DIC drawdown in warm, nitrate-depleted regions, and suggested highest rates of areal N fixation in the North Atlantic, with peaks in each basin in the subtropical gyres. Deutsch et al. (in press) estimated the highest rates within the Pacific basin with maximum rates in the eastern tropical Pacific. Our own simulations had highest rates in the northern Indian basin, where high dust flux and substantial denitrification generated favorable conditions. At present there are very few observations in the Indian Ocean and over most of the Pacific basin. The best sampled region by shipboard studies is in the North Atlantic, where Capone et al., (2005) estimated a mean N fixation by *Trichodesmium* of ~ 87 mmolN/m^2/yr. Our simulations for cases 1 and 6 give similar or slightly higher values for the tropical North Atlantic, but much lower values farther north (Figure 4). Preliminary work suggests that allowing the diazotrophs to access dissolved organic phosphorus improves our simulations in the North Atlantic, but has little impact

elsewhere, and thus would not change our main conclusions here. Cases 1 and 6 also match the observed surface and sub-surface N* values fairly well in the Atlantic basin (Figures 5 and S4).

Negative feedbacks that act to stabilize the ocean N cycle arise via different paths, which we broadly characterize into two groups: uncoupled and coupled. First, there are mechanisms whereby a perturbation to an individual N source/sink will be self-damped; for example in Case 1 (Figure 2), Pacific denitrification decreases with time following the initial pulse independent of any changes in N fixation in the basin simply because overlying surface nitrate concentrations, and thus export production, are lowered. Both coupled and uncoupled feedbacks are illustrated in the Indian basin in Case 1 whereby the rapid rise in N fixation balances the enhanced denitrification after about 100 years. As discussed earlier, the coupled feedbacks can occur on a range of timescales from rather short for surface water N/P to longer for changes in ocean N inventory.

We can quantify the strength of negative uncoupled feedbacks (F_{total}) in our simulations by comparing peak imbalance (I_{max} in Tg N/yr) between N fixation and denitrification with the ending imbalance (I_{end}), where:

$$F_{total} = \frac{(I_{\max} - I_{end})}{I_{\max}}$$

F_{total} would be 1.0 with a perfect negative feedback that returned the N-cycle to net zero balance; an ocean with no stabilizing feedbacks would have a value of 0.0. We subtract 6.7 TgN/yr from the maximum and ending imbalances to account for the initial imbalance in the control simulation. In Case 1 the negative feedback strength was 0.80 at year 200, increasing to 0.86 at year 430. Case 6 had a similar value (0.81 at year 200). In the Case 5, more Fe-replete experiment, the feedback strength was 0.96, and the initial imbalance was larger (Figure 3). The feedback strength was modest in cases 2 and 3 (0.33 and 0.40, respectively). The feedback response was always weaker in the Pacific, and globally the gap between N fixation and denitrification was always still narrowing at the end of the simulations. Case 4 was unusual due to the artificial limit on denitrification, with a calculated feedback strength of 1.2. The rise in denitrification nearly matched the elevated N fixation, erasing the initial imbalance.

The coupled feedback response ($F_{coupled}$) can be quantified in an integrated sense over our 200 year simulations by comparing the net change in nitrogen inventory (with both denitrification and N fixation responses) to the net change due solely to the initially perturbed component, assuming that the other component of the N cycle remained fixed. For Case 1 for example:

$$F_{coupled} = 1.0 - \frac{\Delta_D - \Delta_N}{\Delta_D}$$

where Δ_D and Δ_N (Tg N) are the perturbations in the global time-integrated denitrification N loss and N fixation gain, respectively. Thus, if N fixation did not respond in any way to the increase in denitrification, the coupled feedback response $F_{coupled}$ would be 0.0, and a perfect, inventory maintaining feedback response would have value 1.0. For Case 1, the integrated feedback response is 0.25, indicating that if N fixation had not increased, the oceans would have lost an additional 25% more N over two centuries. For Case 2, the coupled feedback response is 0.16, and for Case 3 (reversing Δ_D and Δ_N in the above equation) the feedback response is 0.33, and for Case 4 the coupled feedback response is 0.26, and for Case 6 it was 0.29. Note that the strength of the integrated feedbacks are weaker than at the end of simulation (F_{total} above). This is due to the timescales of the negative feedbacks, which are not instantaneous but take several decades to centuries. For cases 5 and 6 the situation is more complicated as both denitrification and N fixation were perturbed. Calculating the Case 5 coupled feedback as for Case 1 above gives a value of 0.48, indicating that the oceans would have lost an additional 48% more N if N fixation had remained constant. This again highlights the stronger negative feedback response in the more iron-replete ocean (comparing Cases 1 and 5).

Additional References

Anderson, L. A., and J. L. Sarmiento, 1994. Redfield ratios of remineralization determined by nutrient data analysis. Global Biogeochem. Cycles, 8: 65-80.

Armstrong, R. A., C. Lee, J. I. Hedges, S. Honjo, and S. G. Wakeham, 2002. A new, mechanistic model for organic carbon fluxes in the ocean based on the quantitative association of POC with ballast minerals, *Deep-Sea Res*., Part II, 49, 219–236.

Coles, V.J., Hood, R.R., Pascual, M., Capone, D.G., 2004. Modeling the impact of *Trichodesmium* and nitrogen fixation in the Atlantic Ocean. J. Geophys. Res., 109, C06007, doi:10.1029/2002JC001754.

Krauk, J.M., Villareal, T.A., Sohm, J.A., Montoya, J.P., Capone, D.G., 2006. Plasticity of N:P ratios in laboratory and field populations of *Trichodesmium* spp., Aquatic Microbial Ecology, 42, 243-253.

Fennel, K., Spitz, Y.H., Letelier, R.M., Abbott, M.R., 2002. A deterministic model for N_2-fixation at the HOT site in the subtropical North Pacific. Deep-Sea Research II, 49, 149-174.

Hood, R.R., Bates, N.R., Capone, D.G., Olson, D.B., 2001. Modeling the effect of nitrogen fixation on carbon and nitrogen fluxes at BATS. Deep-Sea Research II, 48, 1609-1648.

Hood, R.R., Laws, E.A., Armstrong, R.A., Bates, N.R., Brown, C.W., and others, 2006. Pelagic functional group modeling: Progress, challenges, and prospects. Deep-Sea Research II, 53, 459-512.

Le Quéré, C., S.P. Harrison, I.C. Prentice, E.T. Buitenhuis, O. Aumont, and others, 2005. Ecosystem dynamics based on plankton functional types for global ocean biogeochemistry models, Global Change Biology, 11, 2016-2040.

Van Mooy, B.A.S., Keil, R.G., Devol, A.H., 2002. Impact of suboxia on sinking particulate organic carbon: Enhanced carbon flux and preferential degradation of amino acids via denitrificiation. Geochimica et Cosmochimica Acta, Vol. 66, 457-465.

Table S2. Global scale fluxes and inventories from our control simulation (year 2050) and the difference from our six case experiments (Case 1 - Increased Denitrification; Case 2 - No Denitrification; Case 3 - No N fixation; Case 4 - Increased N fixation; Case 5 - Increased denitrification as in Case 1, but forced with estimated last glacial maximum dust deposition; Case 6 - Increased denitrification as in Case 1, but with efficient diazotroph Fe utilization). Results for Case 1 are shown at the end of the simulation (year 430), and at year 200 for comparison with the other simulations. Shown are denitrification and N fixation (TgN/yr), primary production and export production (PgC/yr), atmospheric CO_2 (ppm), oceanic nitrogen inventory (Ninv) (% change during simulation). Also shown are basin scale and global N fixation and denitrification rates from each simulation (all in TgN/yr where Dind, Nind is denitrification and N fixation for the Indian basin, etc...), and the global imbalance (Nimb) between fixation and denitrification.

	Denitr	Nfix	PP	ExpP	AtCO2	Ninv	Dind	Nind	Datl	Natl	Dpac	Npac	Dglobal	Nglobal	Nimb
Control	65	58	48	6.1	276.8	-3.1	16.9	25.2	5.96	12.2	41.9	18.9	64.8	58.1	-7
Case 1 yr430	+96	+52	-4.4	-0.67	+5.5	-6.7	35.9	41.8	18.5	32.7	107	33.2	161.1	109.9	-51
Case 1 yr200	+109	+45	-3.7	-0.58	+4.1	-4.1	39.4	41.3	18.8	29.2	115	30.6	173.4	103.2	-70
Case 2 yr200	-65	-17.2	+0.72	+0.14	-4.0	+1.8	0	15.8	0	7.7	0	15.6	0	40.9	+41
Case 3 yr200	-24	-58	-6.6	-1.0	+7.8	-1.7	3.05	0	0.927	0	36.5	0	40.5	0	-41
Case 4 yr200	+5	+12	+1.2	+0.19	-5.1	+0.28	17.7	14.5	5.51	9.91	47.3	42.7	70.5	69.7	-0.8
Case 5 yr200	+97	+75	-4.3	+0.15	-16	-3.5	16.0	33.3	7.59	14.4	139	81.9	163	133	-30
Case 6 yr200	+125	+58	-2.3	-0.40	+0.14	-4.1	48.3	14.5	20.0	9.91	121	42.7	189	69.7	-120

Auxiliary Figures

Figure S1. Selected global scale fluxes are shown for each case experiment. The first 200 years of Case 1 are plotted for easier comparison. The last 20 years of the control are also shown in each plot.

Figure S2. The N* tracer (= ($[NO_3^-]$ + $[NH_4^+]$) - 16 * $[PO_4^-]$) averaged over sub-euphotic zone depths (103-215m) is plotted over time for each of the case experiments at global and basin scales.

Figure S3. The minimum O_2 concentration within the water column at each location is plotted from the World Ocean Atlas 2001 data, from our control (year 2050) and case experiment simulations (year 200).

Figure S4. Spatial patterns are displayed for the N* tracer (= ($[NO_3^-]$ + $[NH_4^+]$) - 16 * $[PO_4^-]$) averaged over euphotic zone depths (< 103m) for the WOA2001 and each of our case experiments.

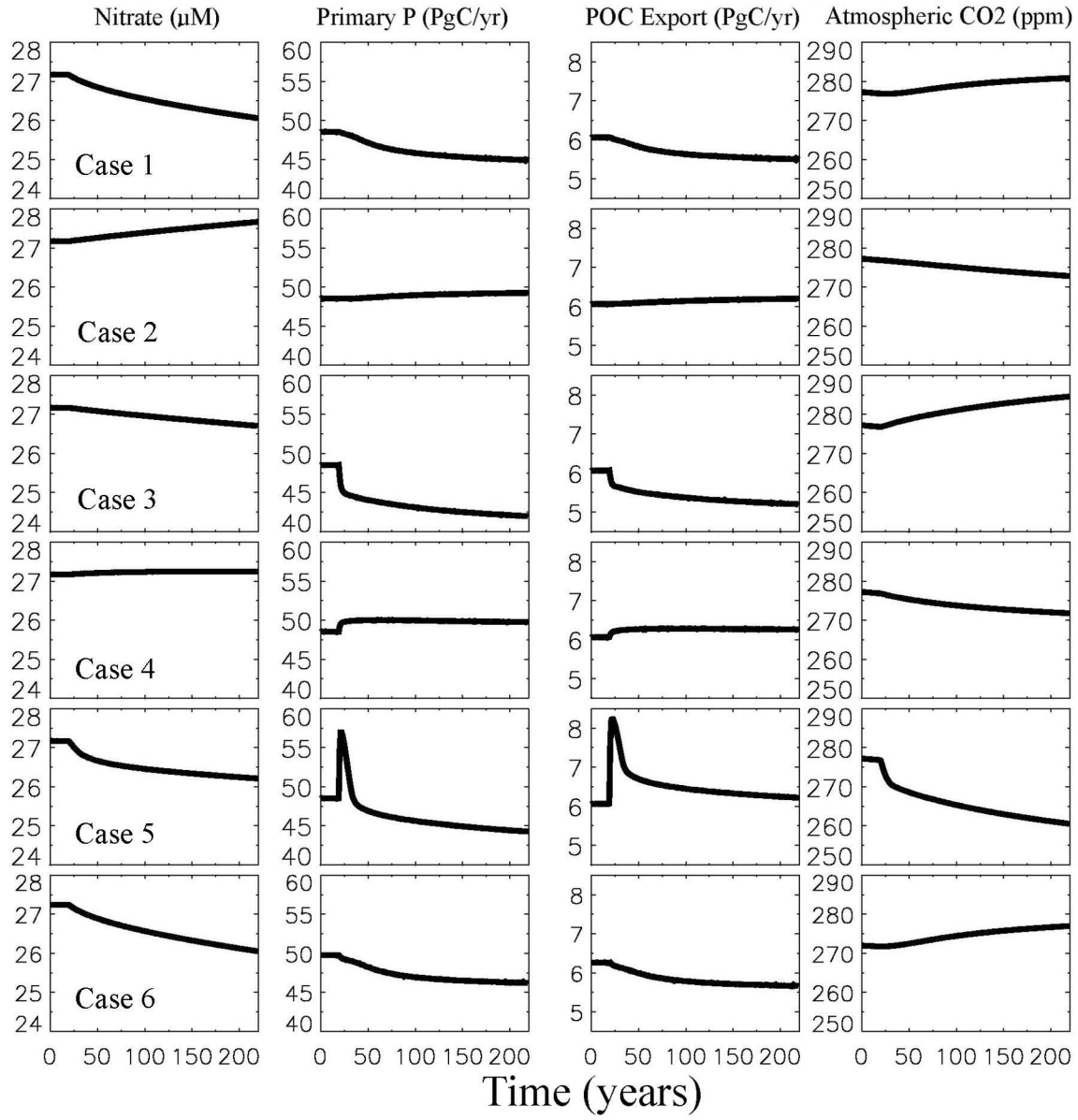
Nitrate (µM)
Primary P (PgC/yr)
POC Export (PgC/yr)
Atmospheric CO2 (ppm)
Case 1
Case 2
Case 3
Case 4
Case 5
Case 6
Time (years)

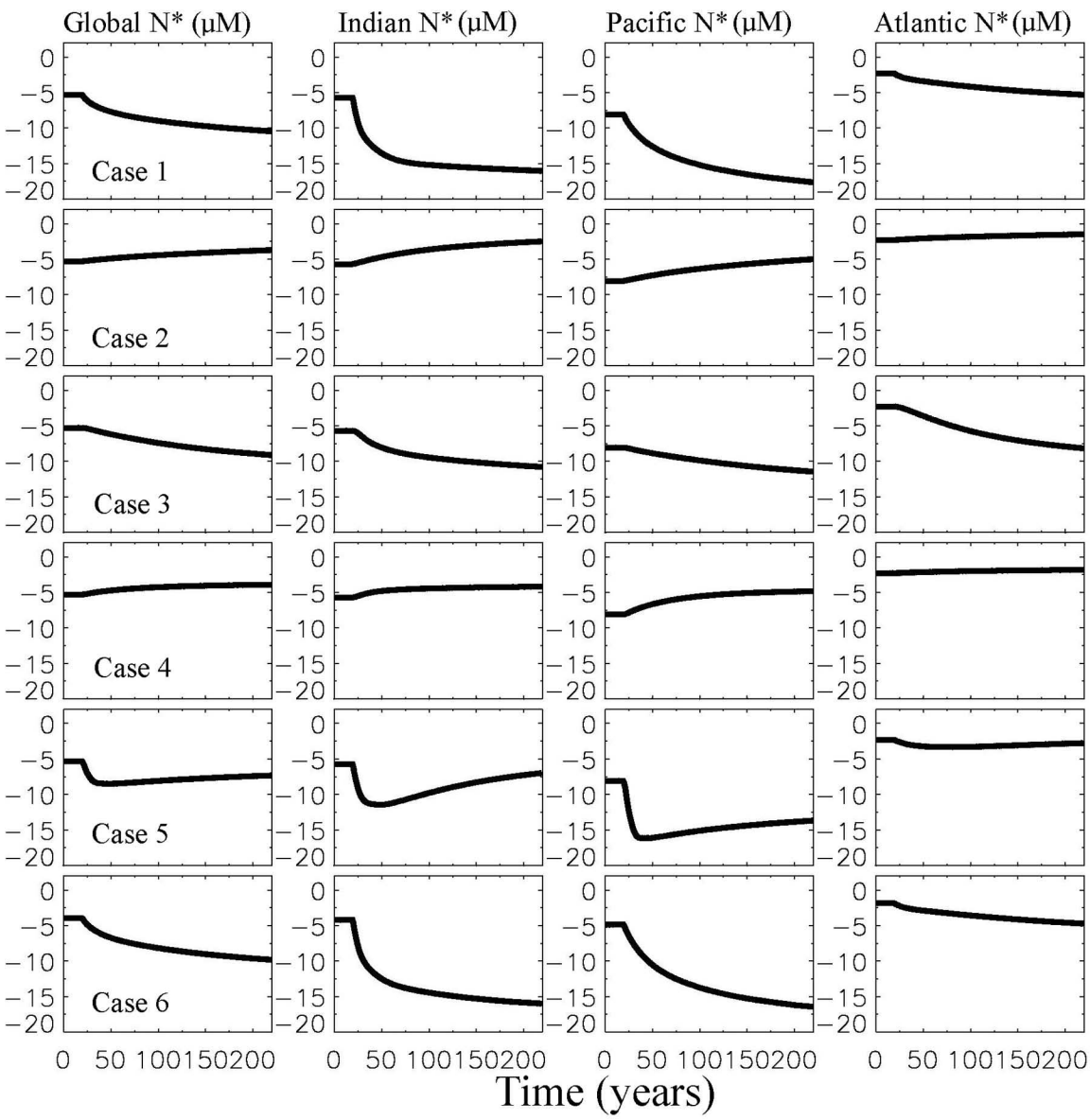
Global N* (μM)
Indian N* (μM)
Pacific N* (μM)
Atlantic N* (μM)
Case 1
Case 2
Case 3
Case 4
Case 5
Case 6
0
−5
−10
−15
−20
0 50 100150200
Time (years)

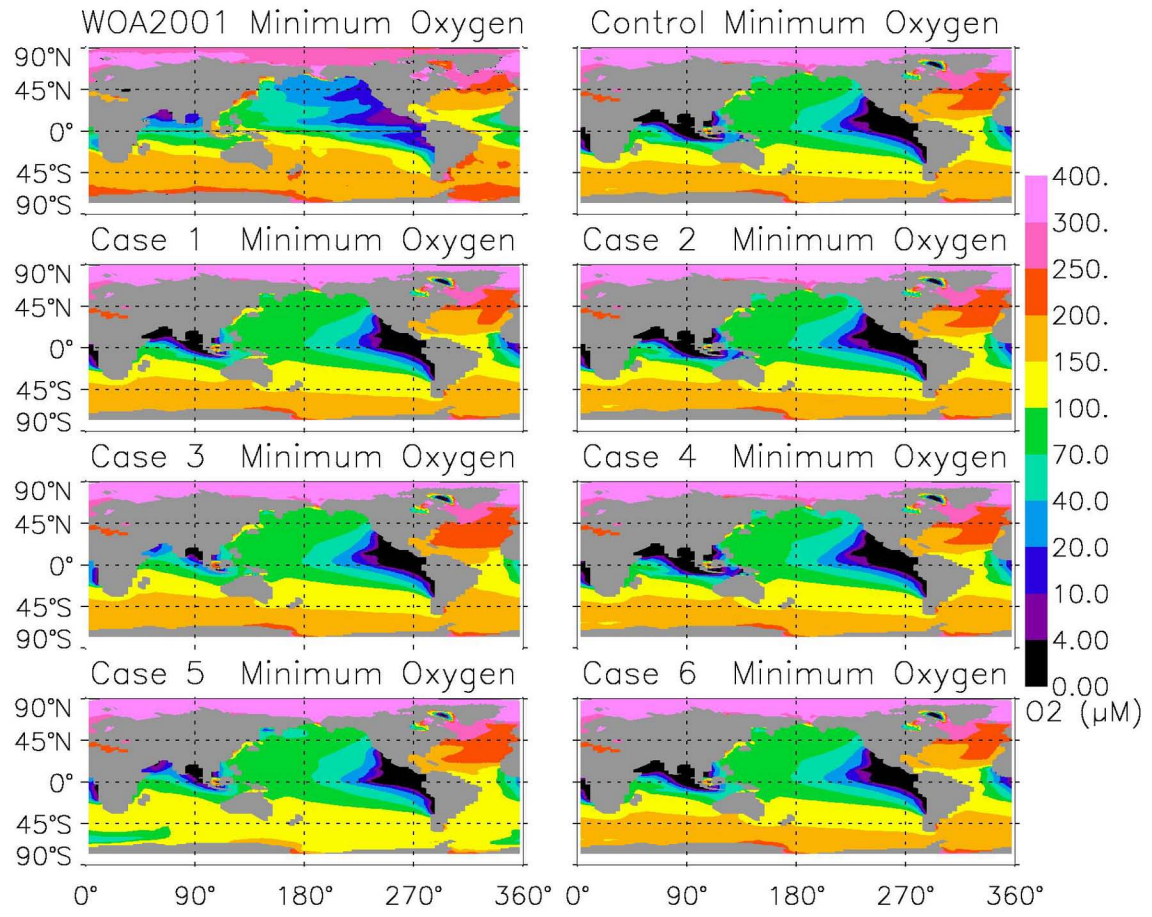
WOA2001 Minimum Oxygen
Control Minimum Oxygen
Case 1 Minimum Oxygen
Case 2 Minimum Oxygen
Case 3 Minimum Oxygen
Case 4 Minimum Oxygen
Case 5 Minimum Oxygen
Case 6 Minimum Oxygen
90°N
45°N
0°
45°S
90°S
0°
90°
180°
270°
360°
400.
300.
250.
200.
150.
100.
70.0
40.0
20.0
10.0
4.00
0.00
O2 (μM)

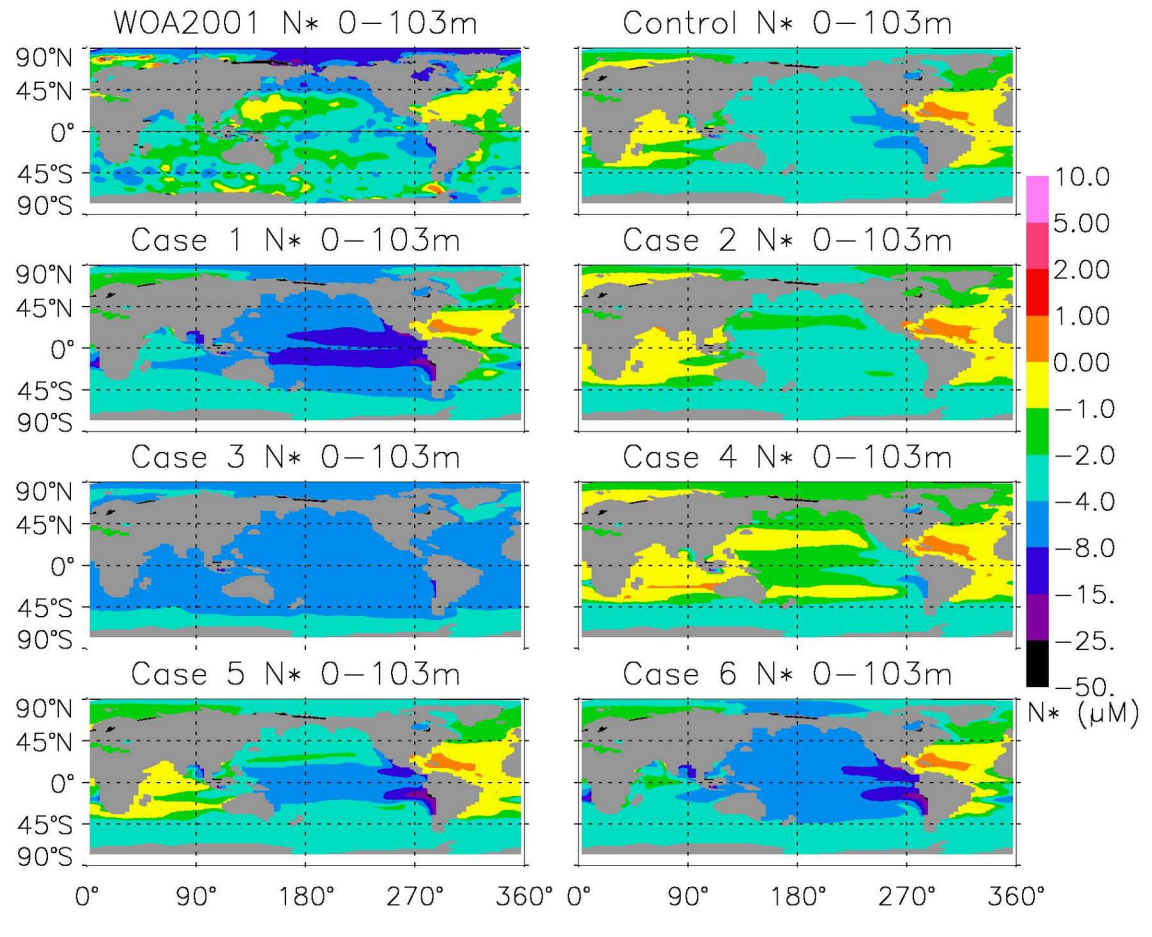
WOA2001 N* 0−103m
Control N* 0−103m
Case 1 N* 0−103m
Case 2 N* 0−103m
Case 3 N* 0−103m
Case 4 N* 0−103m
Case 5 N* 0−103m
Case 6 N* 0−103m
90°N
45°N
0°
45°S
90°S
0°
90°
180°
270°
360°
10.0
5.00
2.00
1.00
0.00
−1.0
−2.0
−4.0
−8.0
−15.
−25.
−50.
N* (μM)